

# Entry, Descent, and Landing Systems Short Course

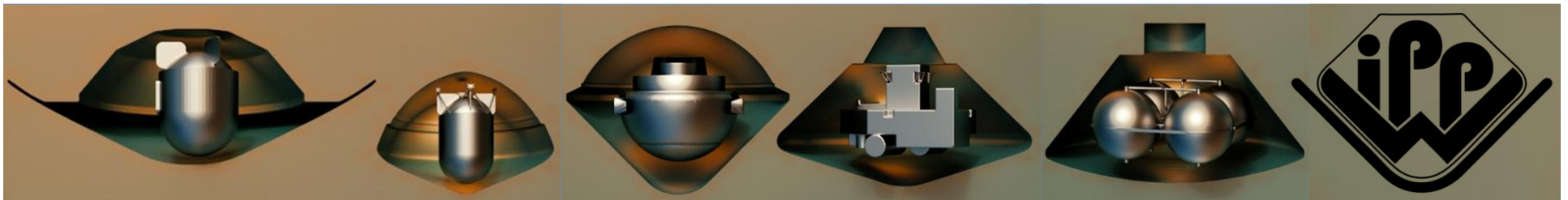
**Subject: Capsule Stability During Planetary Re-Entry**

**Author: L. Ferracina, ATG/ESA**

**Ö. Karatekin, Royal Observatory of Belgium**

With contributions from Sebastien Paris (VKI) & Ali Gülhan (DLR)

sponsored by  
International Planetary Probe Workshop 10  
June 15-16, 2013  
San Jose, California



# Outline



- Stability: a system requirement
- Defining stability: static and dynamic
- A theoretical framework:  
static and dynamic coefficients
- Physics of dynamic instability
- Stability coefficients determination

# Stability: a contradicting requirement



Blunt capsules used in planetary exploration to reduce heating and increasing drag show some “instability” behaviors

Understanding the tendency to fly at a certain attitude is essential for EDLS design

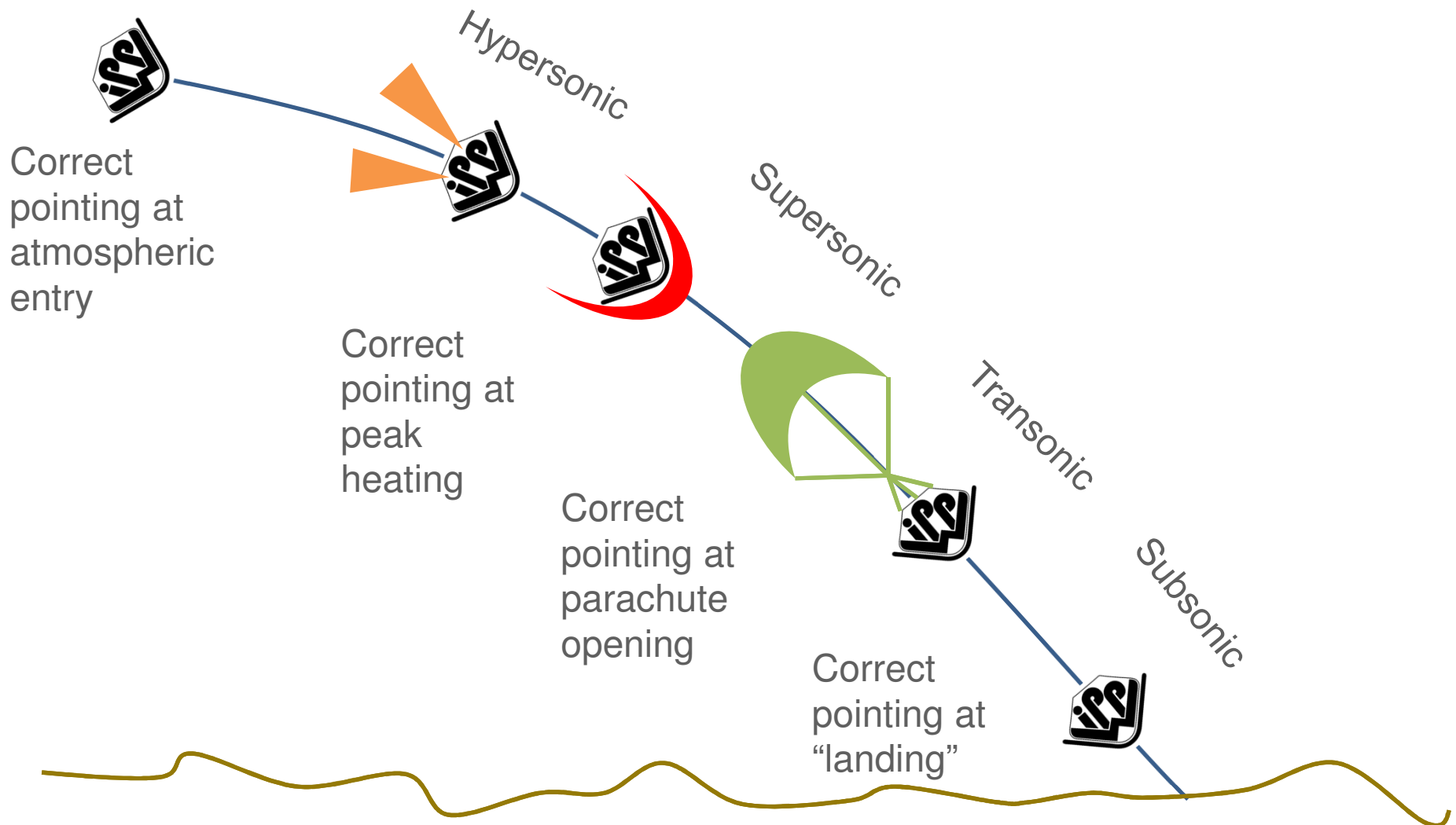
# Stability a system requirement



Capsule stability requirements are strongly linked with

- Entry trajectory type
  - E.g. Hyperbolic trajectory vs Elliptic trajectory
- Configuration
  - Control
  - Parachute usage
  - TPS sizing
- Flight regime
  - Hypersonic, supersonic, transonic, subsonic
- Scientific requirements

# Correct pointing



June 15-16, 2013

International Planetary Probe Workshop 10  
Short Course 2013

# Unstable flight (Genesis)



<http://www.youtube.com/watch?v=dhCrOdbOUkY>



June 15-16, 2013

International Planetary Probe Workshop 10  
Short Course 2013

# Stability



Capsule stability can be defined as the ability to sustain a specific, prescribed flying attitude.

If the net forces and moments exerted on the capsule are zero, the capsule is in equilibrium.

When the capsule is perturbed from its equilibrium position, it may or may not return to its original position.

**Static** and **dynamic stability** quantify if and how the capsule will return to its original position

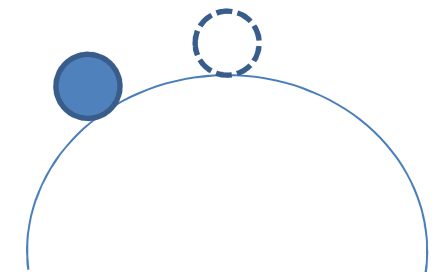
# Static stability



A capsule is (aerodynamically) **statically (or positive) stable** when, following some disturbance from its equilibrium position, the (aerodynamic) forces and moments (acting on it) tend *initially* to return it to the original position.

On the contrary, if the capsule has the tendency to continue in the direction of the displacement then it is **statically unstable (or negative stable)**

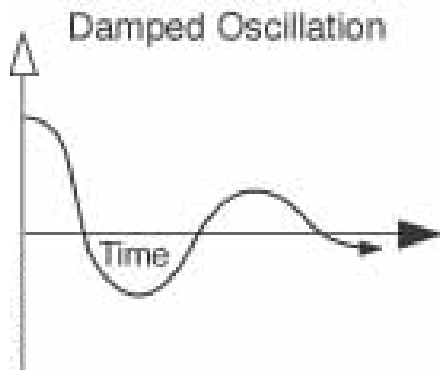
It is **neutrally stable** if it has a tendency to neither return to the equilibrium not to continue in the direction of the movement



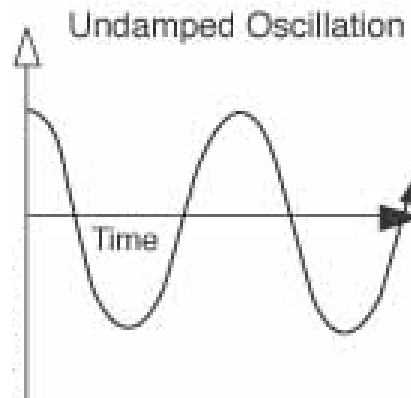
# Dynamic stability



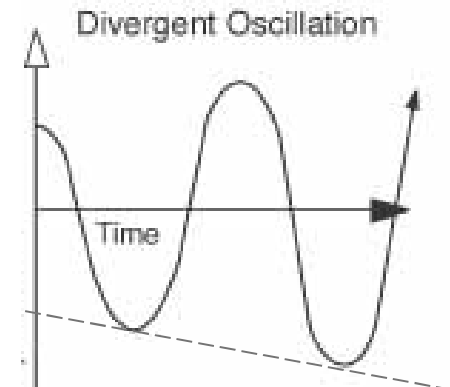
**Dynamic stability** describes whether the angular oscillations are increasing or decreasing over time



**Dynamic stable**  
(positive dynamic stability)



**Dynamic neutral**



**Dynamic unstable**  
(negative dynamic stability)

Remark: dynamic stability



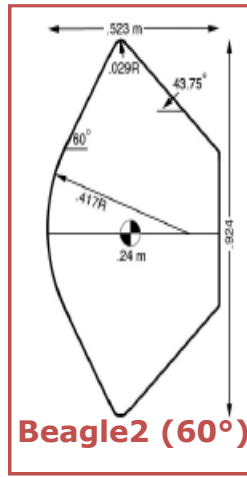
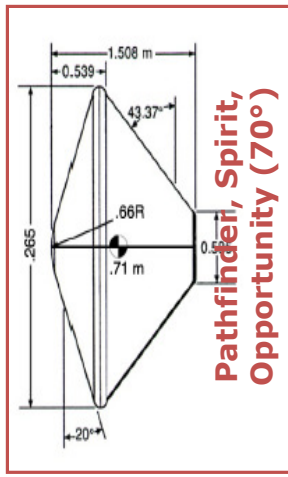
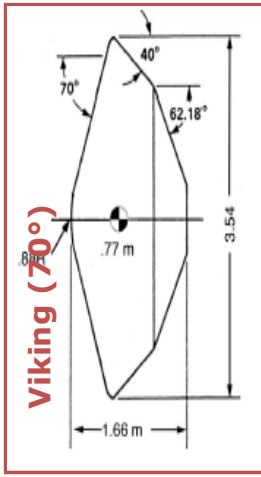
static stability

# Key parameters effecting stability

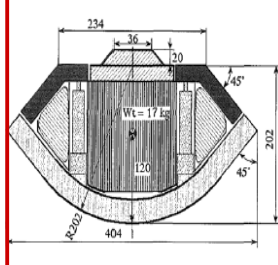


- **Shape (change)**  
e.g.: sharp elongated shapes are more stable than blunt bodies  
Forebody shape, afterbody shape, shoulder radius
- **Mass properties**  
e.g.: forward center of gravity improve stability
- **Environment/flying conditions**  
e.g.: a capsule that is stable at supersonic regime can be unstable at subsonic one
- **Roughness**  
e.g.: rough surfaces enhance laminar to turbulent transition that effect dynamic stability

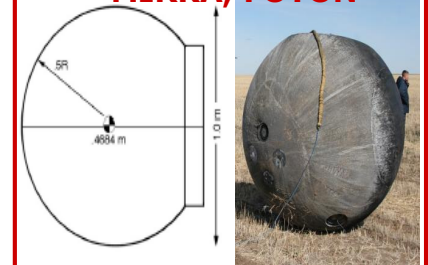
# A large diversity



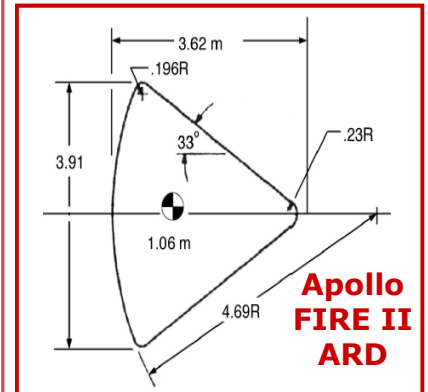
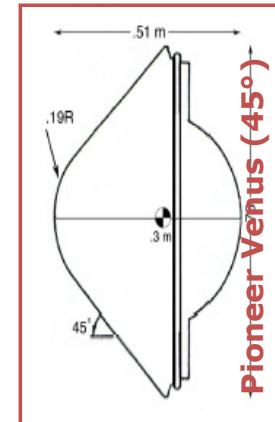
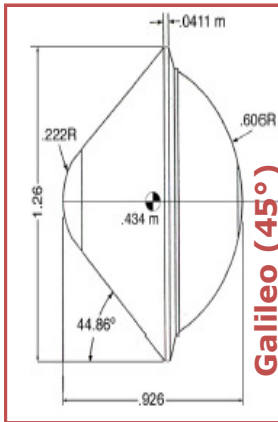
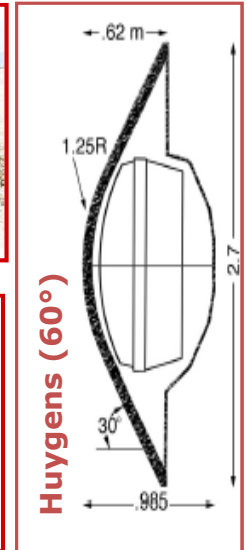
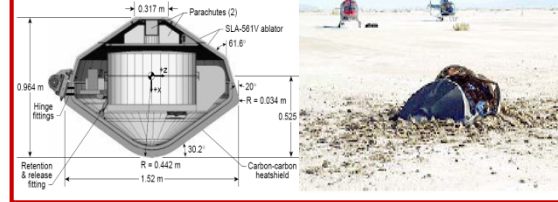
**Hayabusa (45°)**



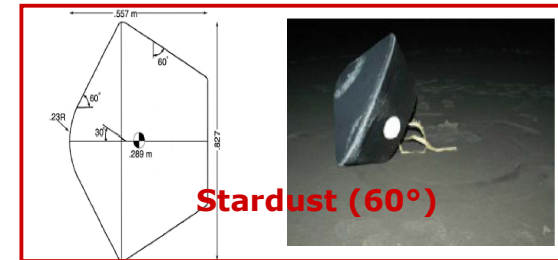
**MIRKA, FOTON**



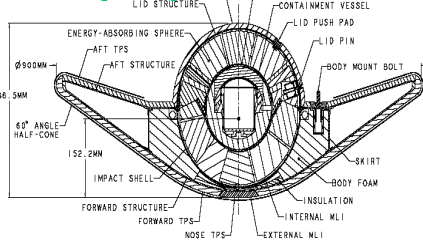
**Genesis (60°)**



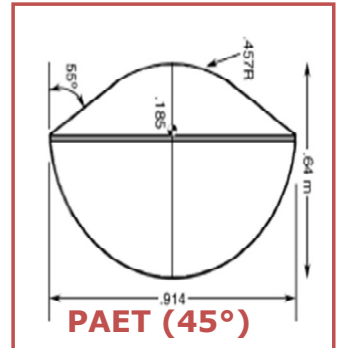
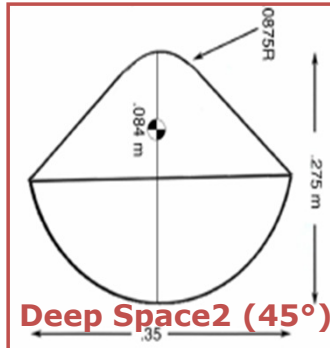
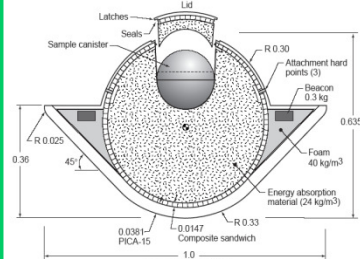
**Stardust (60°)**



**MSR (60°)**



**MSR (45°)**



# Reference System



$R=N+A=L+D$  : Resultant

N: Normal Force

A: Axial Force

L: Lift

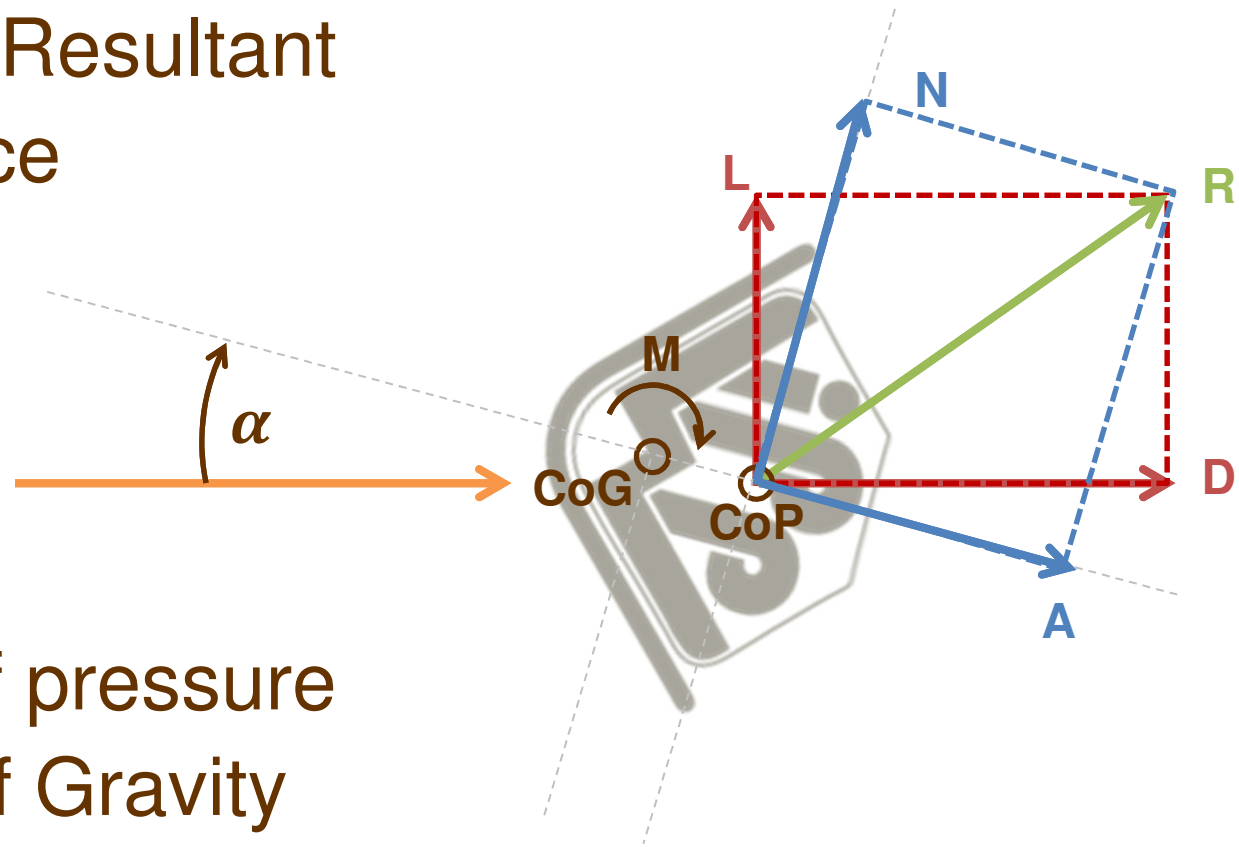
D: Drag

M: Momentum

CoP: Center of pressure

CoG: Center of Gravity

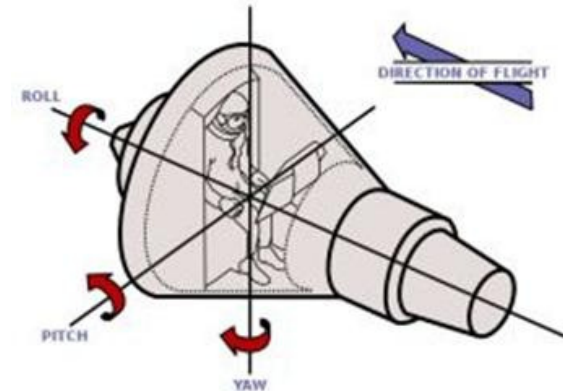
$\alpha$ : Angle of attach (AoA)



# Condition for static stability



- For a positive variation of the angle of attack  $d\alpha$ , the momentum  $dM$  must be negative  $\frac{dM}{d\alpha} < 0$



For fully axis symmetric capsule yaw=pitch and it is simply called (total) angle of attack ( $\alpha$ )

- It is usually measured by the variation of the pitch moment coefficient  $C_M = \frac{M}{q_\infty A l}$  with the angle of attach

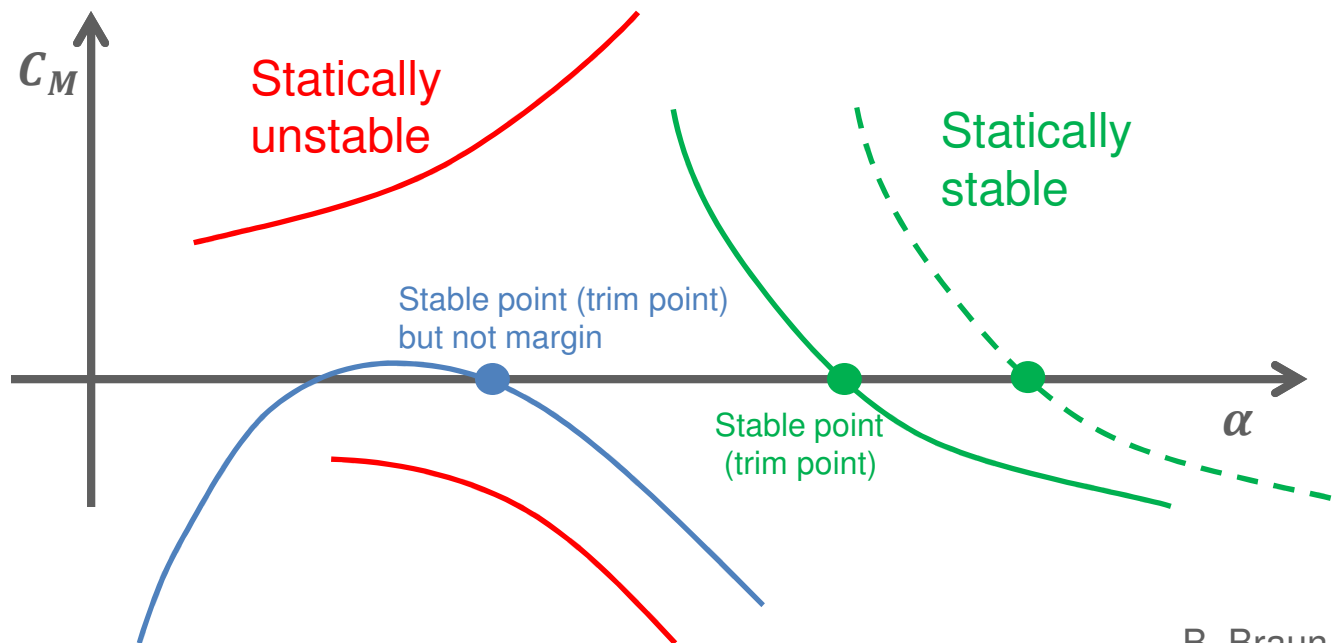
$$\frac{dC_M}{d\alpha} < 0 \quad \text{Static stability condition}$$

# $\frac{dC_M}{d\alpha} < 0$ is not sufficient



In addition to a negative slope ( $\frac{dC_M}{d\alpha} < 0$ )

- Trim (stable) point
- Sufficient margin around that point



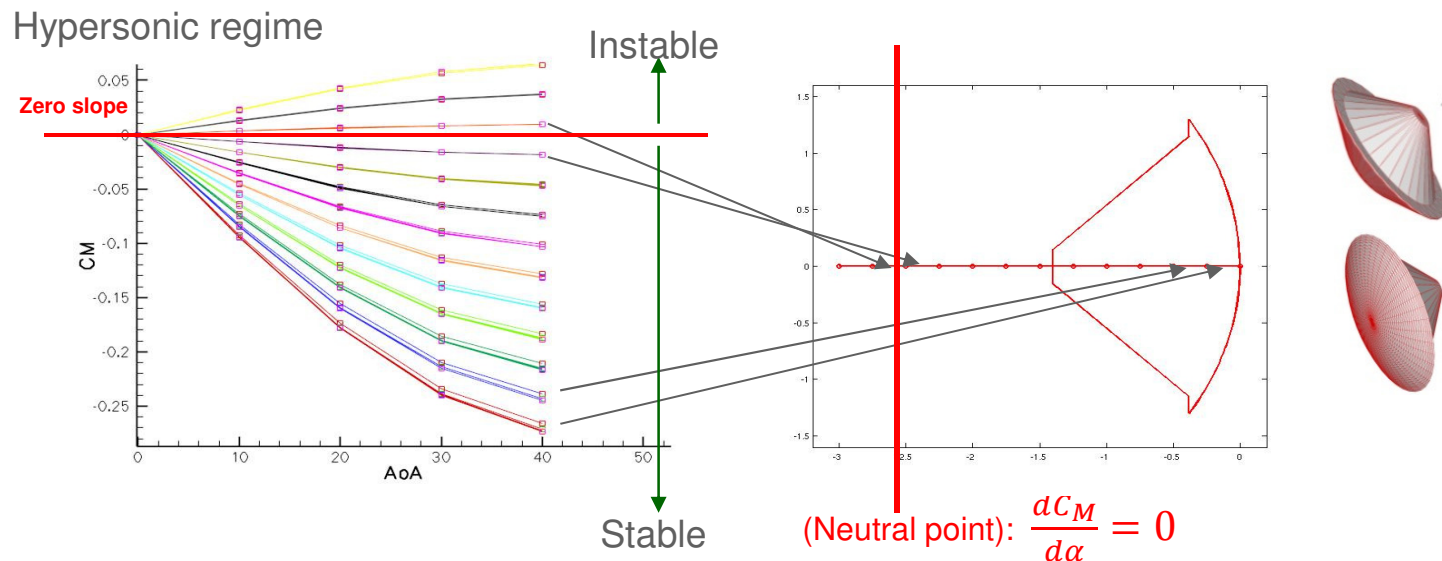
B. Braun EDL course

# Static Margin



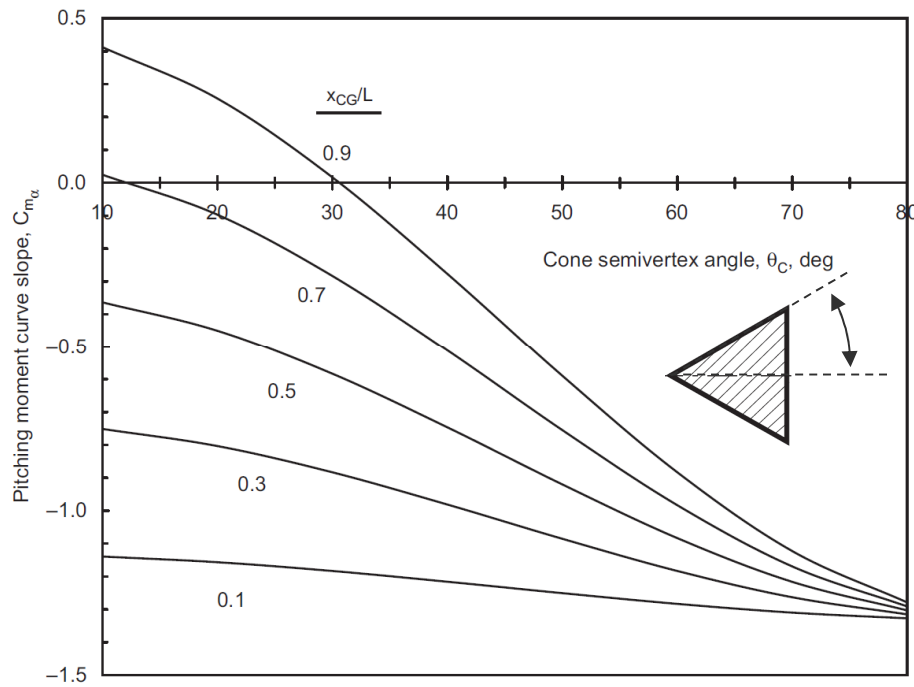
The pitching moment  $C_M = \frac{M}{q_\infty Al}$

- is a function of the angle of attack  $\alpha$  and of Mach number
- is defined for a specific point (usually the CoG but for blunt capsule is often the nose or the axial position of the maximum diameter)



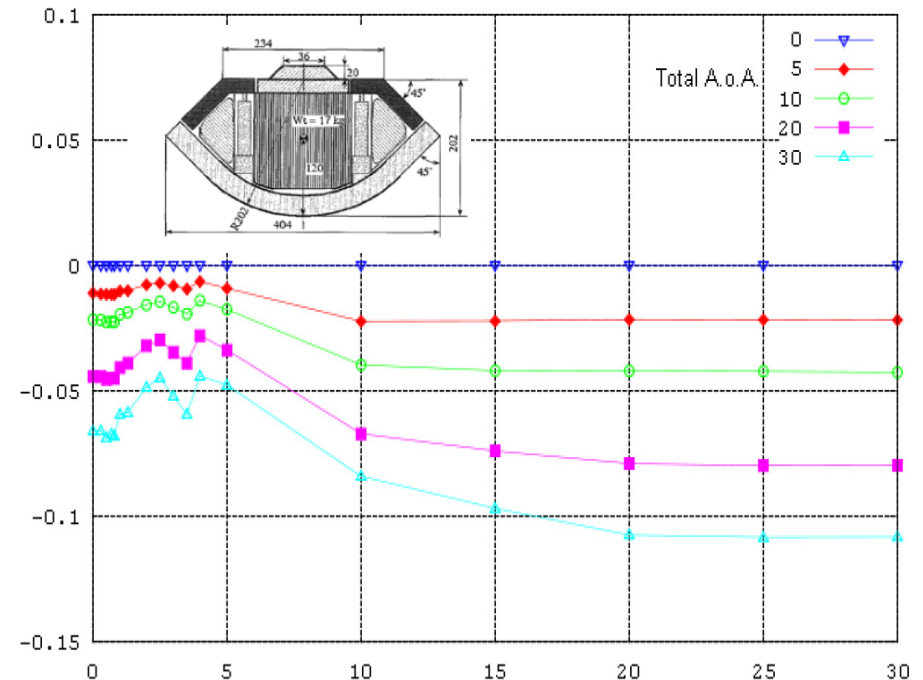
The distance between the Neutral Point and the CoG is called the **Static Margin**

# Shape, Mach, $\alpha$ , CoG dependency



Notes on Earth Atmospheric Entry for Mars Sample Return Mission T. Rivell

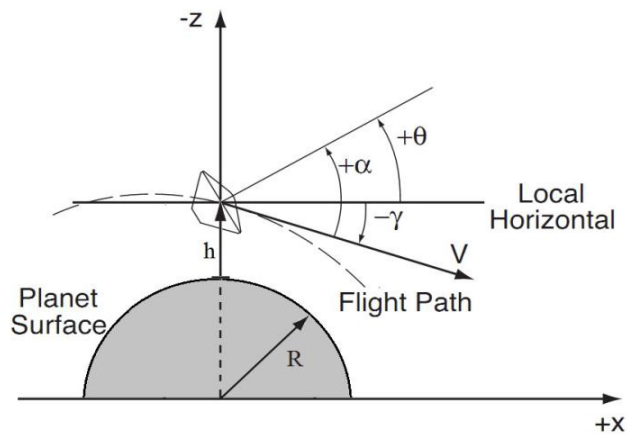
Moving the CoG forward and a larger cone semi-vertex angle improve static stability (hypersonic, Newtonian approximation)



Attitude Motion and Aerodynamic Characteristics of MUSES-C Reentry Capsule, N. Ishii et al.

$C_M$  at different regimes (from hypersonic to subsonic) for different angle of attach  $\alpha$

# Planar motion analysis



Survey of Blunt Body Dynamic Stability in Supersonic Flow AIAA 2012-4509

- Motions are restricted to a plane
- Spherical non rotating planet
- Gravitational field constant
- Small L/D
- Constant mass
- No wind
- Aerodynamic coefficients independent on Mach and linearized with

$\alpha$ : Angle of attach  
 $\gamma$ : Flight path angle  
 $\theta$ : Pitch angle  
 $q = \dot{\theta}$ : Pitch rate  
 $V$ : Velocity  
 $h$ : Altitude  
 $R$ : planet radius  
 $S$ : Reference Surface

$D$ : Diameter  
 $C_L$ : Lift coefficient  
 $C_D$ : Drag coefficient  
 $C_M$ : Momentum Coefficient  
 $C_{M\dot{\alpha}} = \frac{\partial C_M}{\partial \left(\frac{\dot{\alpha}D}{V}\right)}$   
 $C_{Mq} = \frac{\partial C_M}{\partial \left(\frac{\dot{\theta}D}{V}\right)}$

$$\frac{dh}{dt} = \dot{h} = V \sin \gamma$$

$$\dot{V} = -\frac{\rho V^2 S C_D}{2m} - g \sin \gamma$$

$$\dot{\gamma} = \frac{\rho V S C_L}{2m} - \left(\frac{g}{V} - \frac{V}{R}\right) \cos \gamma$$

$$\dot{\theta} = \frac{\rho V^2 S d}{2I} \left( C_{m_q} \frac{\dot{\theta}d}{2V} + C_{m_{\dot{\alpha}}} \frac{\dot{\alpha}d}{2V} + C_{m_{\alpha}} \alpha \right)$$

# Obtaining a 2<sup>nd</sup> ODE



$$\ddot{\theta} = \frac{\rho V^2 S d}{2I} \left( C_{m_q} \frac{\dot{\theta} d}{2V} + C_{m_{\dot{\alpha}}} \frac{\dot{\alpha} d}{2V} + C_{m_{\alpha}} \alpha \right)$$

$$\theta = \alpha + \gamma$$

$$\dot{\theta} = \dot{\alpha} + \dot{\gamma} = \dot{\alpha} + \frac{\rho V S C_L}{2m} \quad C_{m_q} \frac{\dot{\theta} d}{2V} = C_{m_q} \left( \frac{\dot{\alpha} d}{2V} + \frac{\rho S d C_L}{4m} \right)$$

$$\ddot{\theta} = \ddot{\alpha} + \frac{d}{dt} \left( \frac{V \rho S C_L}{2m} - g \sin \gamma \right) = \ddot{\alpha} + \dots$$

$$\ddot{\alpha} + \left( \frac{\rho V S}{2m} \right)^2 C_D C_{L_{\alpha}} \alpha + \frac{\rho V S}{2m} C_{L_{\alpha}} \dot{\alpha} = \frac{\rho V^2 S d}{2I} \left( C_{m_q} \frac{\dot{\theta} d}{2V} + C_{m_{\dot{\alpha}}} \frac{\dot{\alpha} d}{2V} + C_{m_{\alpha}} \alpha \right)$$

$$\ddot{\alpha} - \frac{\rho V S}{2m} \left( -C_{L_{\alpha}} + \frac{m d^2}{2I} (C_{m_q} + C_{m_{\dot{\alpha}}}) \right) \dot{\alpha} - \frac{\rho V^2 S d}{2I} C_{m_{\alpha}} \alpha = 0$$

# A dynamic stability indicator



## Equation

$$\ddot{\alpha} - \frac{\rho V S}{2m} \left( -C_{L\alpha} + \frac{md^2}{2I} (C_{m_q} + C_{m_{\dot{\alpha}}}) \right) \dot{\alpha} - \frac{\rho V^2 S d}{2I} C_{m_\alpha} \alpha = 0$$

is of the form  $\ddot{\alpha} + A\dot{\alpha} + B\alpha = 0$  and can be solved explicitly. The solution is

$$\alpha = Ae^{\xi_1 t} \cos(\omega t + \delta)$$

$$\xi_1 = \frac{\rho V S}{4m} \left( -C_{L\alpha} + \frac{md^2}{2I} (C_{m_q} + C_{M_{\dot{\alpha}}}) \right)$$

Indication of  
dynamic stability

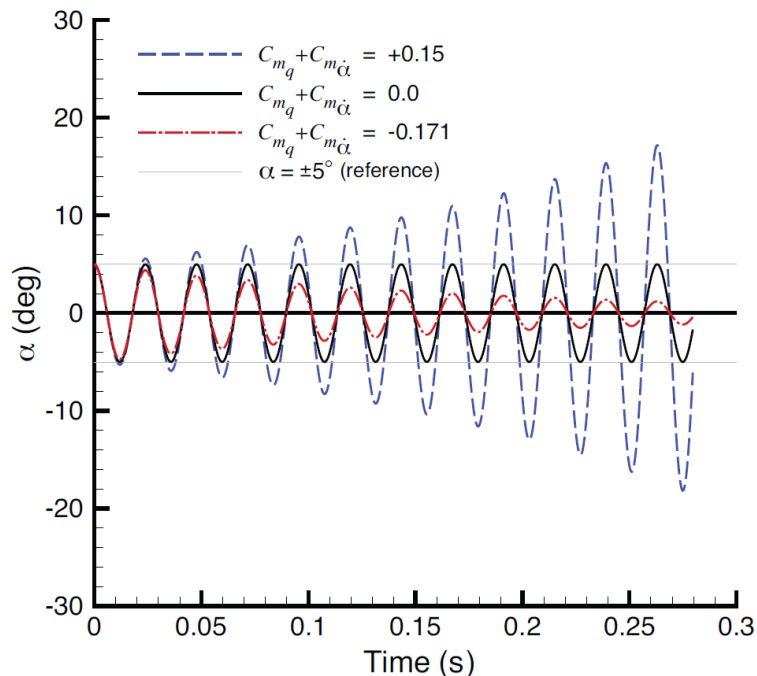
$$\omega = \sqrt{-\frac{\rho V^2 S d}{2I} C_{m_\alpha}}$$

# An example: free to tumble



$$\ddot{\alpha} - \frac{\rho V S}{2m} \left( -\cancel{C_{L\alpha}} + \frac{md^2}{2I} (C_{m_q} + C_{m_{\dot{\alpha}}}) \right) \dot{\alpha} - \frac{\rho V^2 S d}{2I} C_{m_\alpha} \alpha = 0$$

$$\alpha = Ae^{\xi_1 t} \cos(\omega t + \delta) \quad \xi_1 = \frac{\rho V S d^2}{8I} (C_{m_q} + C_{m_{\dot{\alpha}}}) \quad \omega = \sqrt{-\frac{\rho V^2 S d}{2I} C_{m_\alpha}}$$



NASA Mercury Space Capsule— Winds of Change  
 NASA Langley Research Center 1/22/1959 Image # EL-1996-00094

Limit Cycle Analysis Applied to the Oscillations of Decelerating Blunt-Body Entry Vehicles. M. Schoenenberger, E. M. Queen

# Dynamic stability criteria

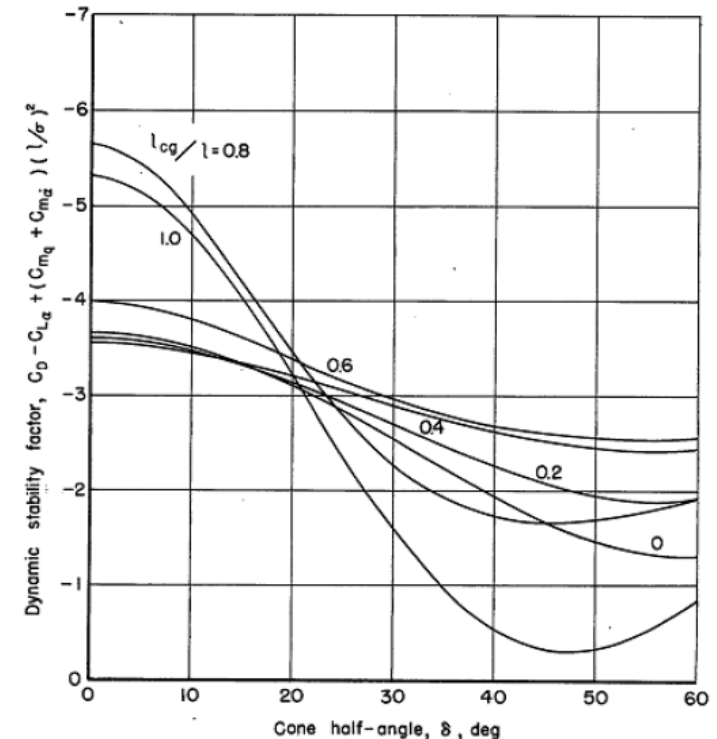


- Dynamic stability is more complex than static one
- Dynamic stability criteria involve static and dynamic coefficients
- A more general dynamic stability coefficient (introducing exponential atmosphere)

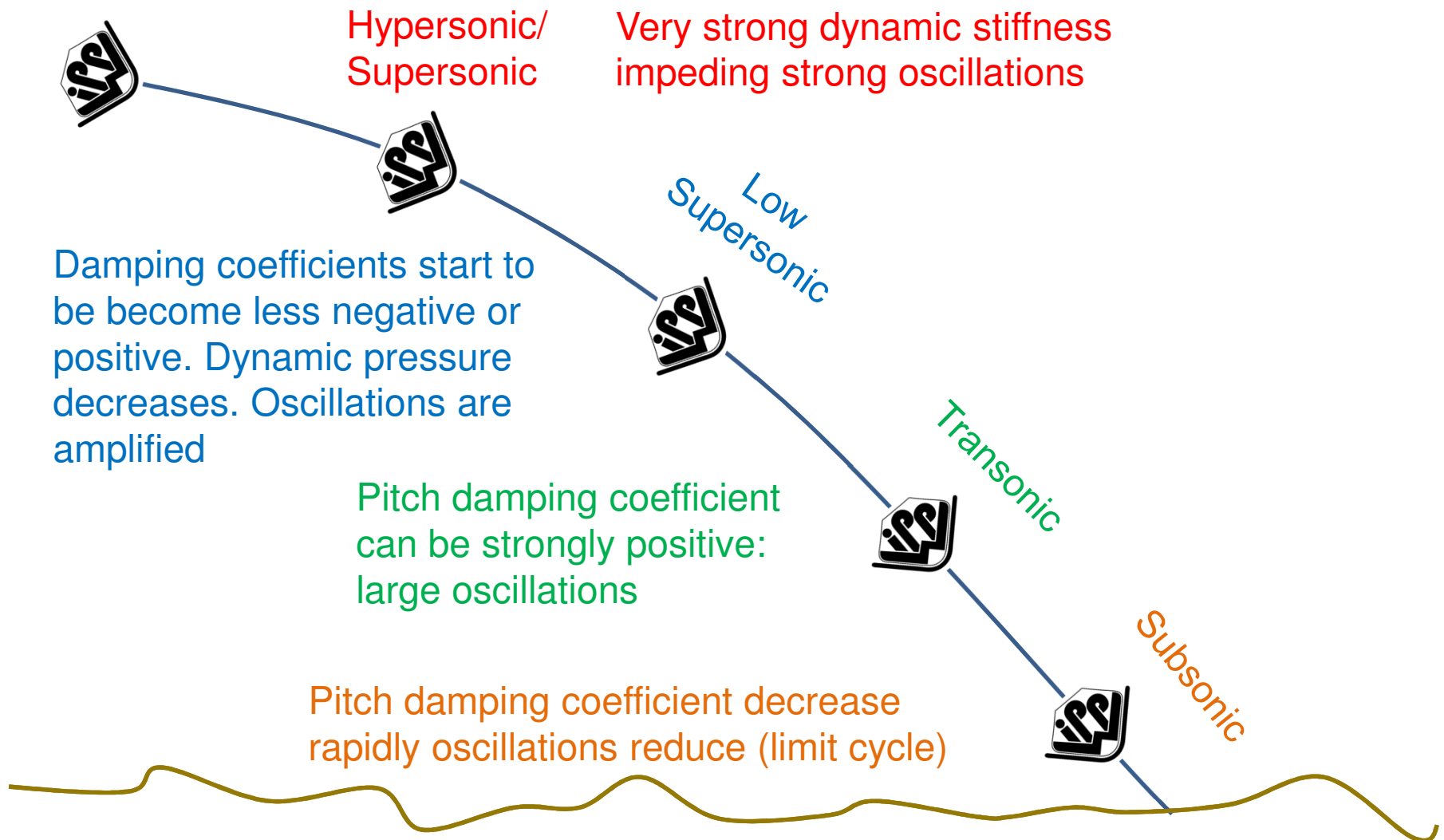
$$\xi = C_D - C_{L\alpha} + \frac{md^2}{2I} (C_{m_q} + C_{m\dot{\alpha}})$$

the vehicle is dynamically stable if  $\xi < 0$

- More commonly the term  $(C_{m_q} + C_{m\dot{\alpha}})$  (pitch damping coefficient) is used independently as a measure of dynamic stability (with  $C_{m_q} + C_{m\dot{\alpha}} < 0$  indicating damping behaviour)



# From entry to touchdown



June 15-16, 2013

International Planetary Probe Workshop 10  
Short Course 2013

# Physics of dynamic instability

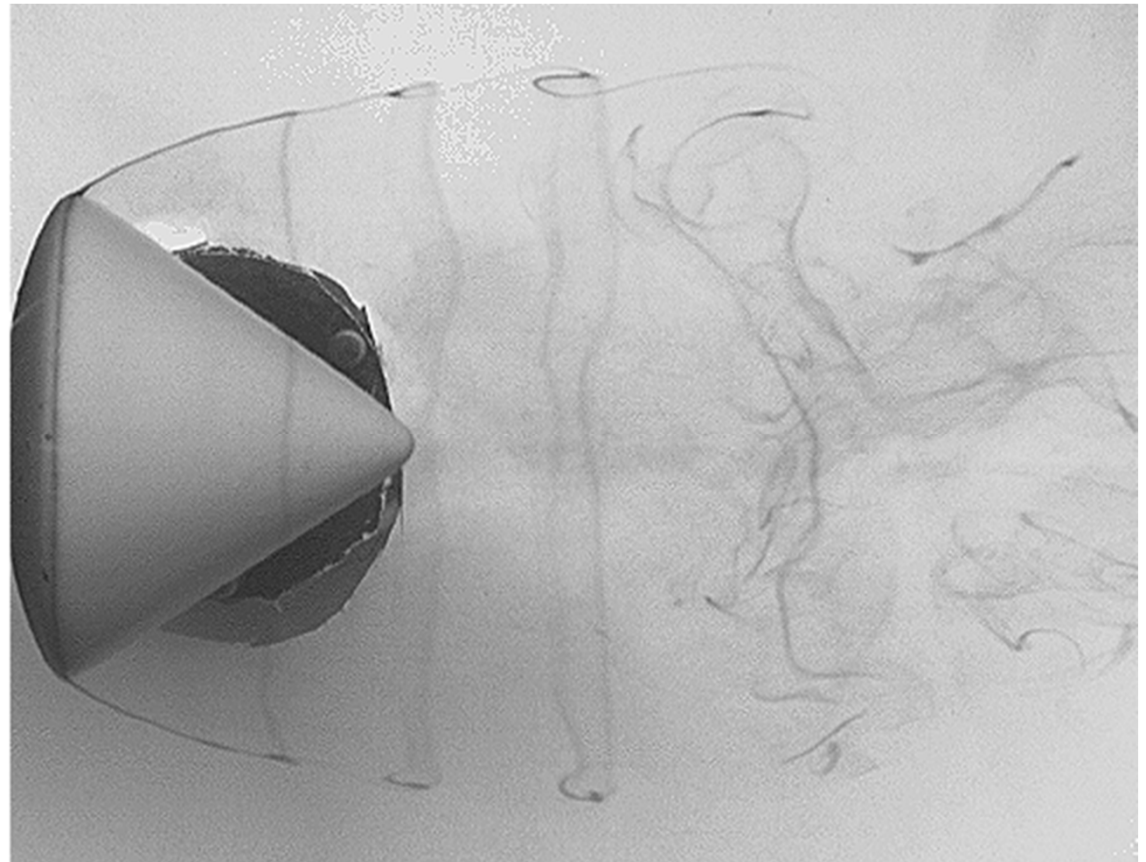
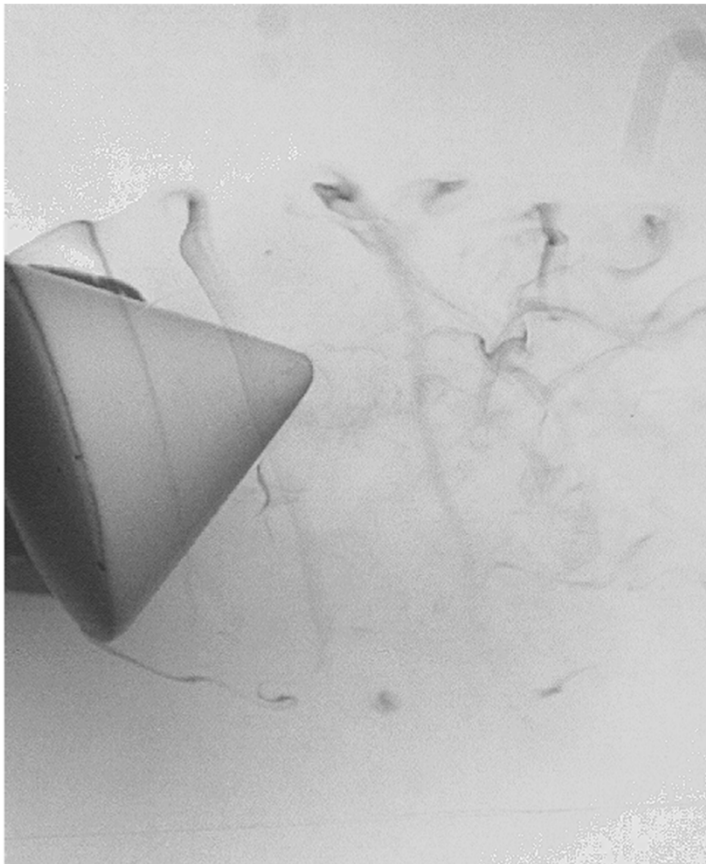


No full and clear understanding is available.

Many parameters have been suggested by different authors as key phenomena:

- Unsteady near wake
- Interaction between after-body geometry and wake
- Surface flow separation/reattachment
- Time lag between the front part and the aft part of the capsule
- Decreasing dynamic pressure (aerodynamic stiffness)
- Hysteresis
- ...

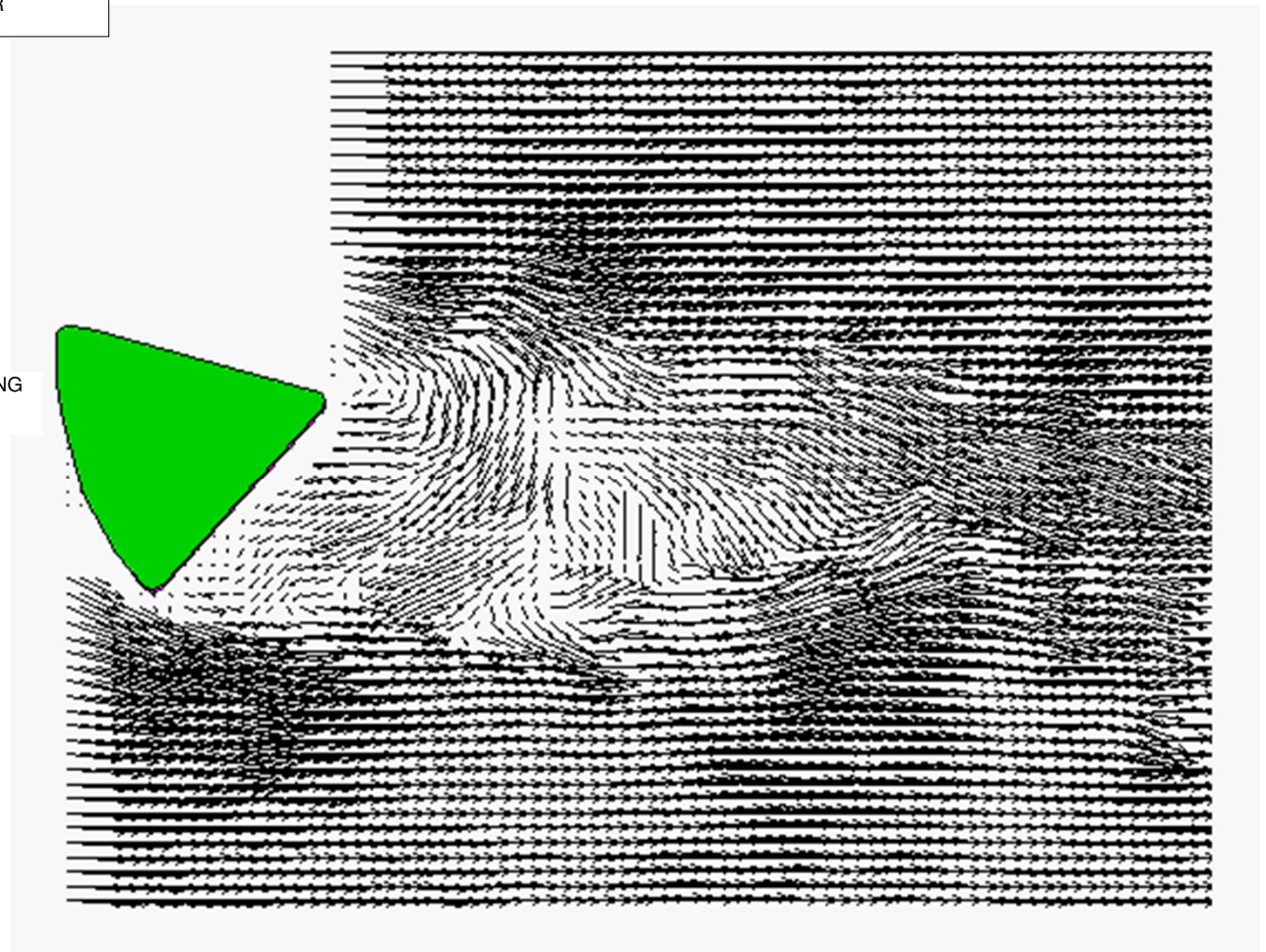
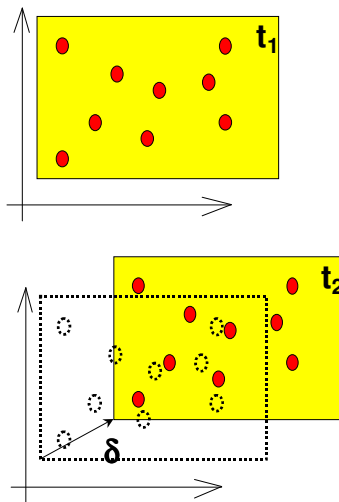
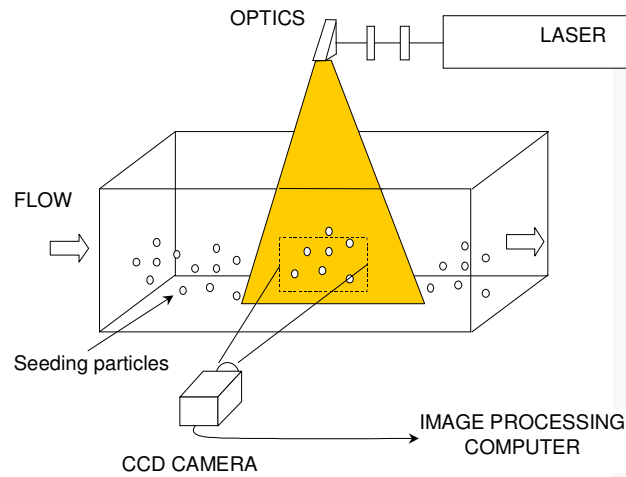
# Unsteady near the wake (Dye flow visualization in water WT)



June 15-16, 2013

International Planetary Probe Workshop 10  
Short Course 2013

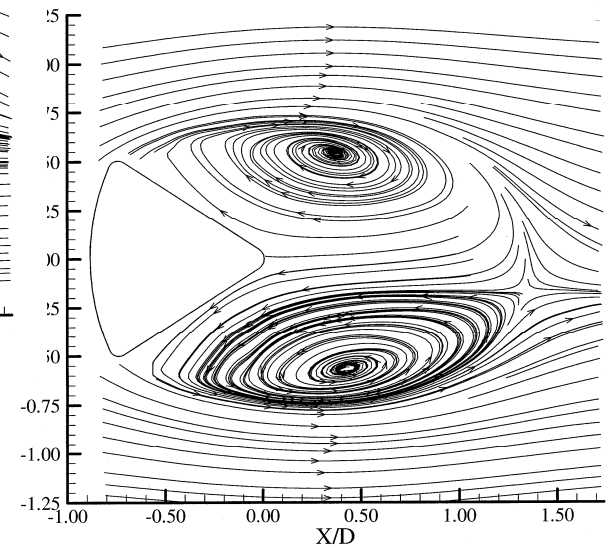
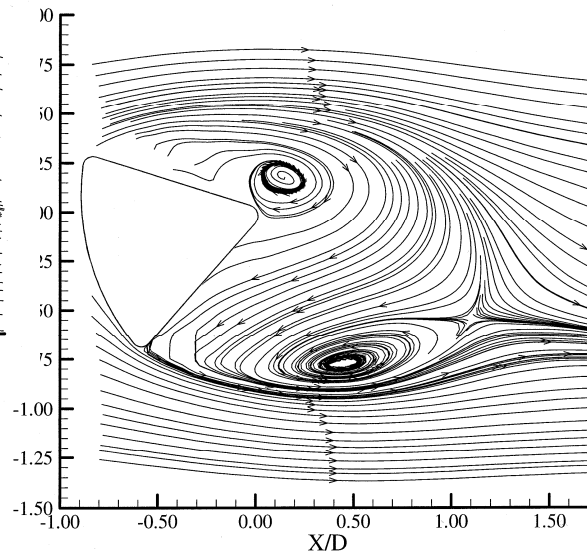
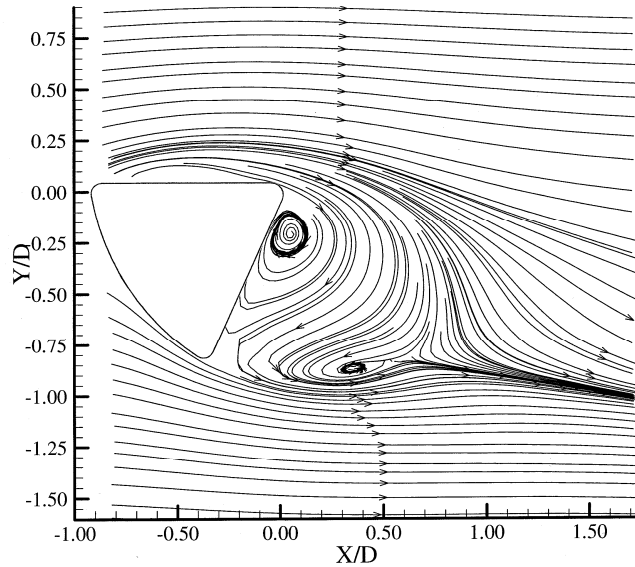
# Unsteady near the wake (PIV visualization in water WT)



June 15-16, 2013

International Planetary Probe Workshop 10  
Short Course 2013

# LDV (Laser Doppler Velocimetry) Mean flow in the symmetry plane



June 15-16, 2013

International Planetary Probe Workshop 10  
Short Course 2013

# Stability coefficient determination



	Analytical	Computational	Experimental
Static coefficient	Close analytical form (Newton method like for simple shapes)	DSMC Newton method like CFD: Euler / (RA)NS LES (DNS)	Captive tests
Dynamic coefficients	Close analytical form	DSMC Newton method like CFD: Euler / U(RA)NS LES (DNS)	Free flight: <ul style="list-style-type: none"><li>• Ballistic ranges</li><li>• Drop tests</li></ul> Captive test <ul style="list-style-type: none"><li>• Free oscillation</li><li>• Free to tumble</li><li>• Force oscillation</li></ul>

# Computational techniques



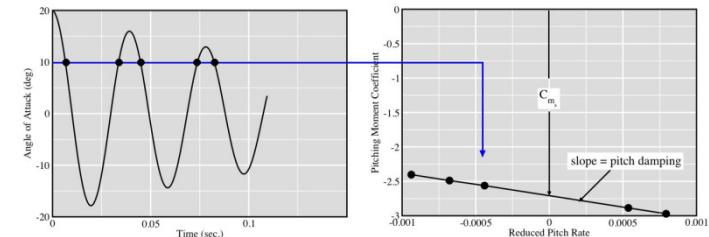
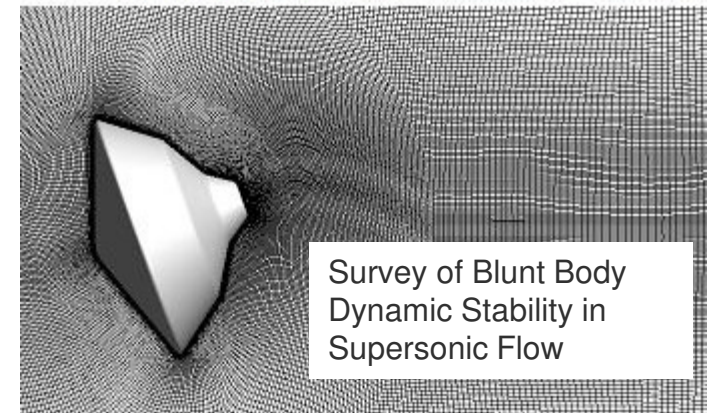
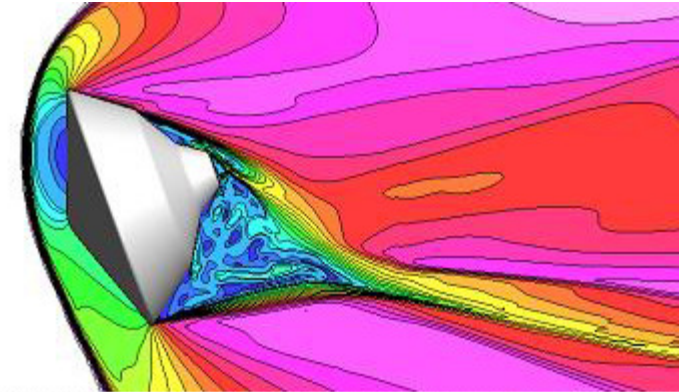
CFD became a key technology in the design process (to complement the experiments or for optimization) and in the reconstruction step

Matured methods for static analysis, in great evolution concerning dynamic stability derivatives determination (time resolved loads computed on a moving-body)

(U)RANS, LES and FSI are continuously improving in terms of accuracy, detailed level and computational power.

CFD has been shown to be useful for static aerodynamic coef estimations. But is generally accepted within the community that current computational tools cannot accurately predict the pitch damping coefficient which is required for a quantitative assessment of the dynamic oscillation growth.

Currently static coefficients can be predicted using the CFD, However the current computational tools cannot accurately predict the pitch damping coefficient which is required for a quantitative assessment of the dynamic oscillation growth



# Ballistic ranges



The model is either shot with a pneumatic or ballistic gun or simply cut free and allowed to fall (balloon)

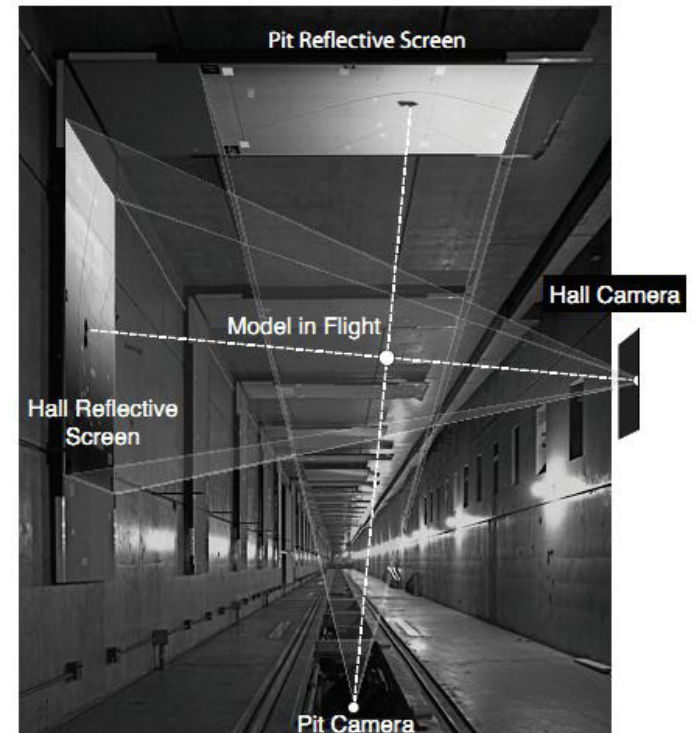
The model is observed with schlieren photography, high speed video, or embedded instrumentation to extract pitching behavior

## Advantages:

- Full 6 DoF behavior (support free)
- Perfect similitude in Mach and density.

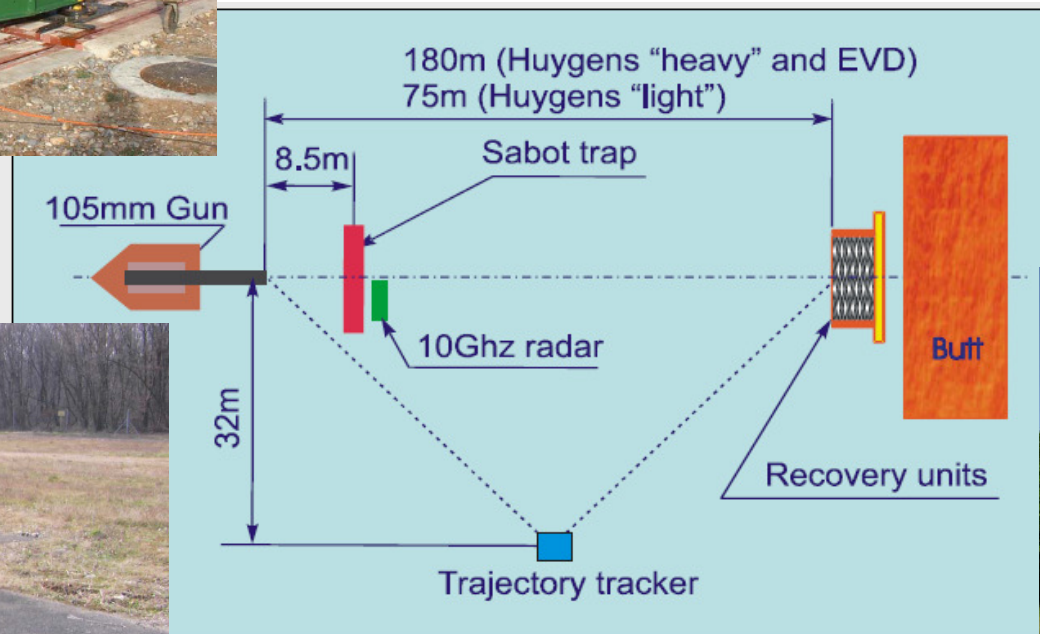
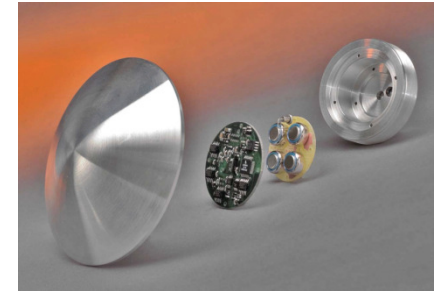
## Disadvantages

- Dynamic scaling (mass, Mol Mach, Reynolds Strouhal, numbers) is critical
- Delicate reconstruction procedure
- Not ideal for lifting bodies.



Schlieren imaging station at Eglin AFB  
Aeroballistic Research Facility

# Aerothermodynamics of Aerocapture and High Speed Earth Entry



June 15-16, 2013

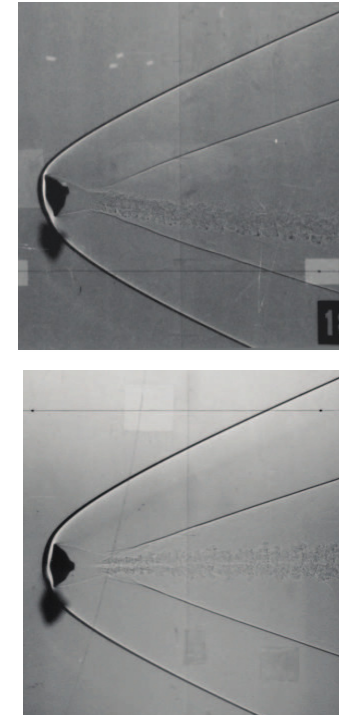
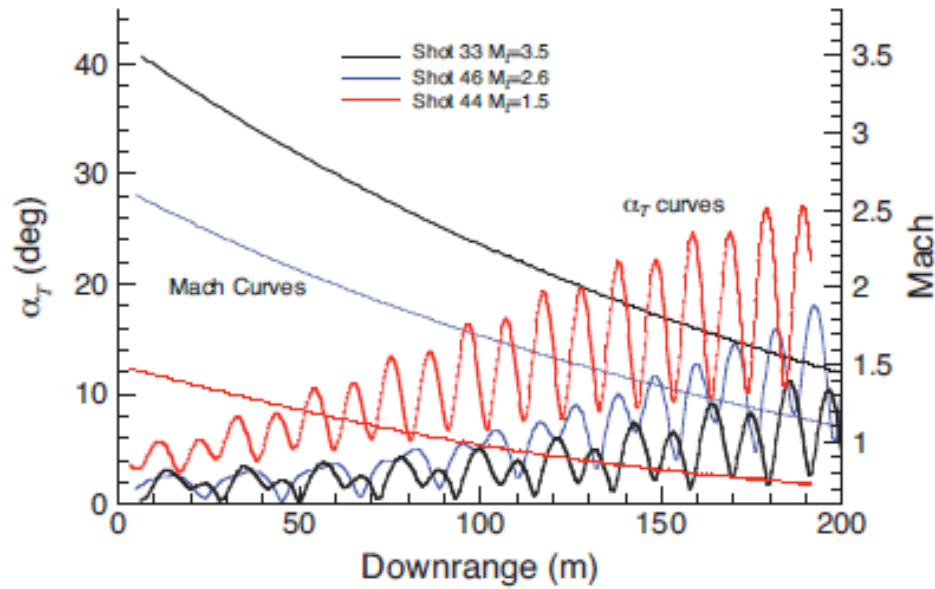
International Planetary Probe Workshop 10  
Short Course 2013

# ISL test campaign



June 15-16, 2013

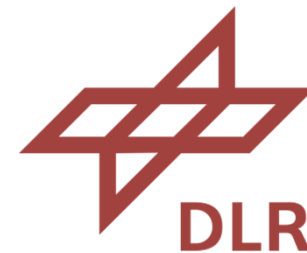
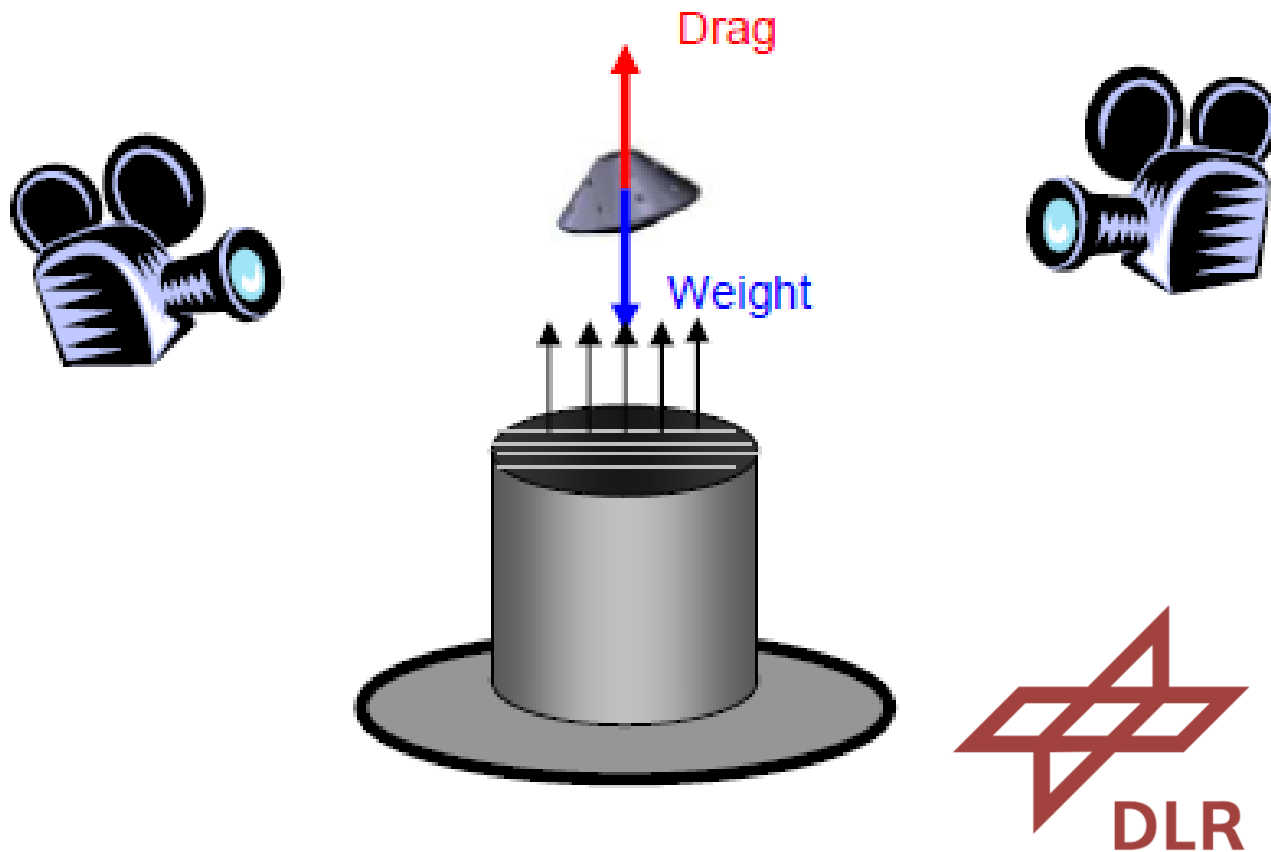
# Ballistic Tests



Example of amplitude growth with initial Mach number of MSL Ballistic tests (Schoeneberger et al. 2009)

Shadowgraphs of MSL Ballistic tests  $M=2.7$ ,  $a=13$   $B=0$  (Schoeneberger et al. 2009)

# Marco Polo R dynamic stability



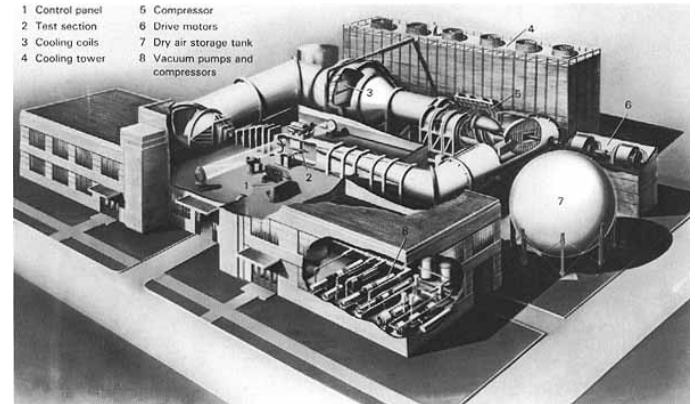
June 15-16, 2013

International Planetary Probe Workshop 10  
Short Course 2013

# Capitive Tests: Wind Tunnels



VKI L1 tunnel, Belgium



6x6 ft Wind tunnel at NASA Ames Research Center



Gemini capsule testing, NASA



Small-scale model of the Crew Exploration Vehicle at Ames Research Center.

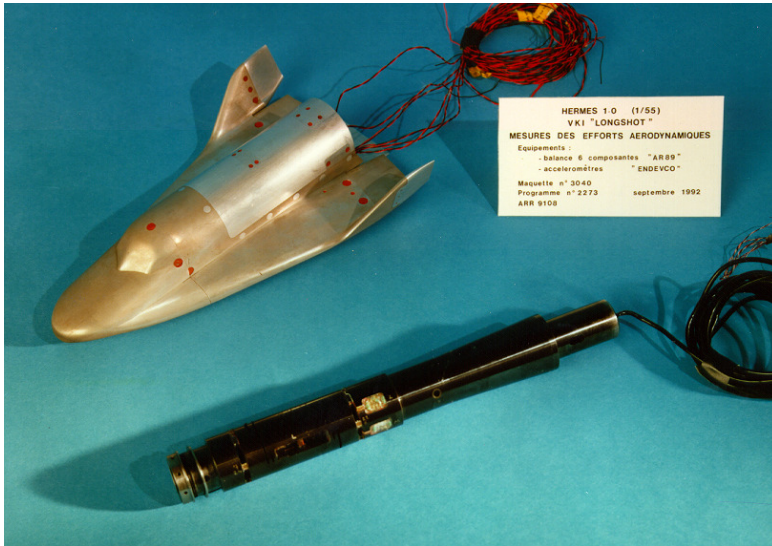


F-111B tests at NASA Ames

Wind tunnels allow to characterize in detail the flow field, aero-thermodynamic forces and the dynamical response of the vehicles at a given upstream flow conditions

6/15/2013

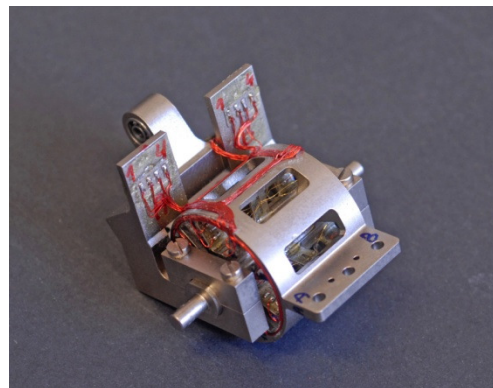
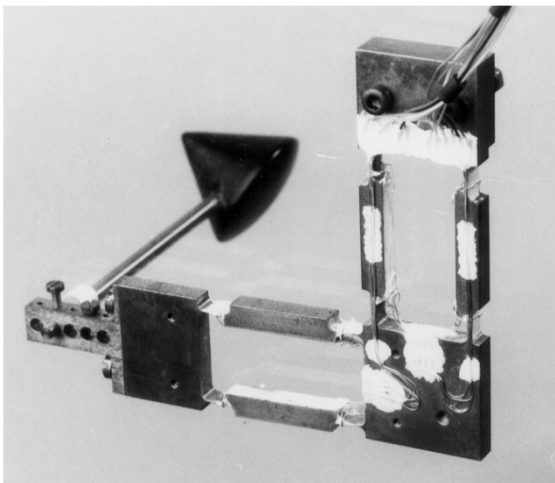
# Static tests



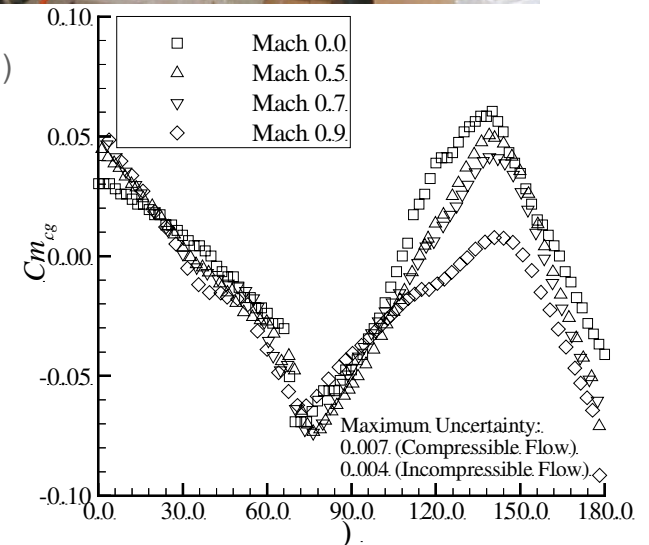
HERMES 1.0 (1/55)  
VKI "LONGSHOT"  
MESURES DES EFFORTS AERODYNAMIQUES  
Equipements :  
- balance 6 composantes "AR89"  
- accéléromètres "ENDEVCO"  
Maquette n° 3040  
Programme n° 2273 septembre 1992  
ARR 9108



6 component force balances for VKI Hypersonic Long Shot Tunnel facility (VKI)



3 component force balances for subsonic and transonic facilities (VKI)



Compressibility effects on Apollo moment coefficients (Wang et al. 2000).

# Captive tests 1DoF: Dynamic Stability Coefficients



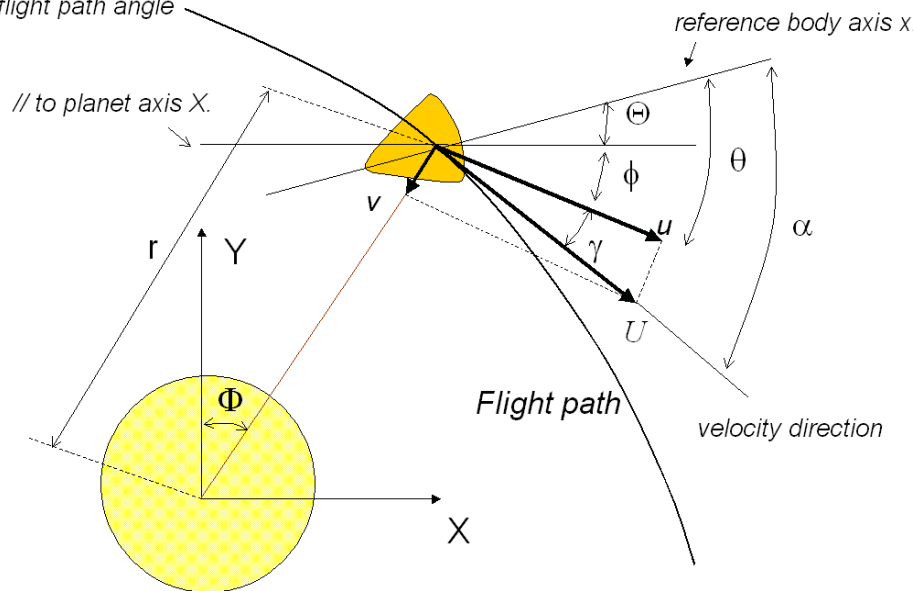
The governing equation in 1DOF in Rotation

$$\underbrace{I\ddot{\theta}}_{\text{Inertia}} - \underbrace{\left(C_{m_q} + C_{m_{\dot{\alpha}}}\right) \frac{q_{\infty}SD^2}{2U_{\infty}} \dot{\theta}}_{\text{Damping}} - \underbrace{q_{\infty}SD \frac{\partial C_m}{\partial \theta}}_{\text{Stiffness}} \theta = \underbrace{M(t)}_{\text{External Moment}}$$

$$C_{m_{\dot{\alpha}}} = \frac{\partial C_m}{\partial \left(\dot{\alpha}D/U_{\infty}\right)} \quad C_{m_q} = \frac{\partial C_m}{\partial \left(\dot{\theta}D/U_{\infty}\right)}$$

- I moment of inertia
- $\theta$  pitch angle
- $\alpha$  angle of attack
- $C_m$  moment coefficient
- $q_{\infty}$  dynamic pressure
- S reference area
- D characteristic length
- $U_{\infty}$  freestream velocity
- M(t) external moment

$\alpha$  = angle of attack.  
 $\gamma$  = flight path angle



In the above equation all (Inertia, static moments) are known except the aerodynamic damping.

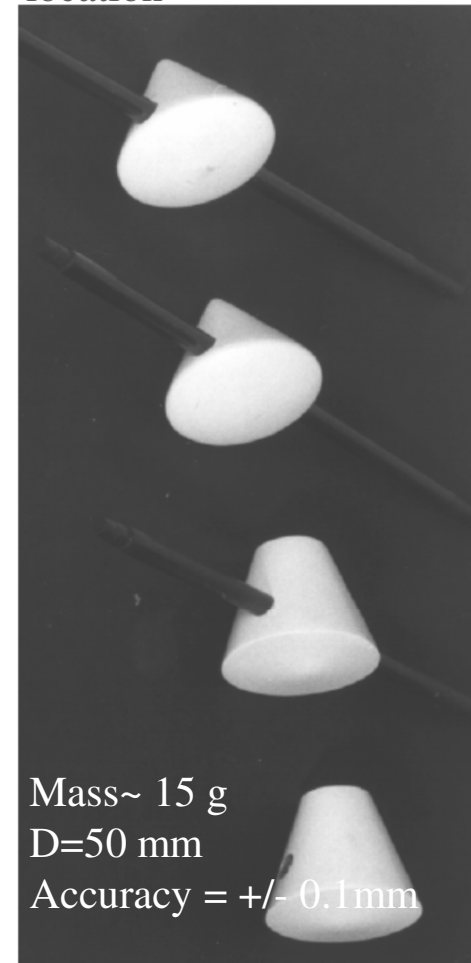
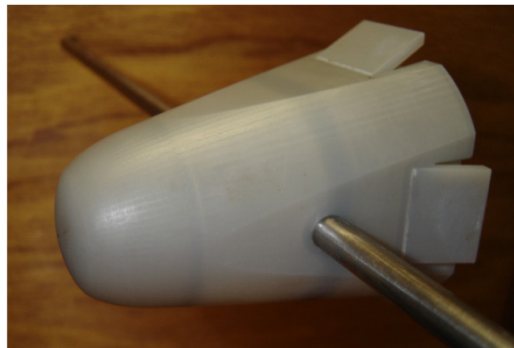
The extracted damping parameter is the combined damping coefficient because it is impossible to separate the angle of attack change from the pitch rate due to the kinematical motion limitations by oscillation round the rotation center.

# Wind tunnel models



- Full scale model tests are rare they occur in low speeds generally.
- Most of the tests, especially at high speeds are done with scaled models.
- These made out of metal/s (Al, Mg, etc.) plexiglas, foam & resin. Supports are usually metal or carbon fiber

- Light models (resin with density  $1.38\text{g/m}^3$ )
- Precision in the CG location



# Similitude Parameters



The natural frequency during the flight (Strouhal number, St) can be deduced from the resolution of the second order differential equation

$$(\omega_n)_{ft} = \sqrt{\frac{q_\infty SD \left| \left( \frac{\partial C_m}{\partial \theta} \right) \right|}{I} - \left( \frac{q_\infty SD (C_{m_q} + C_{m_\alpha})}{2I} \right)^2}_{ft}$$

$$(St)_{ft} = \left( \frac{fD}{U_\infty} \right)_{ft} = \sqrt{\frac{\rho_\infty SD^3 \left| \left( \frac{\partial C_m}{\partial \theta} \right) \right|}{8\pi^2 I}}_{ft}$$

In order to reproduce the dynamic behavior of the vehicle, the flight and experimental “Strouhal number” have to be similar

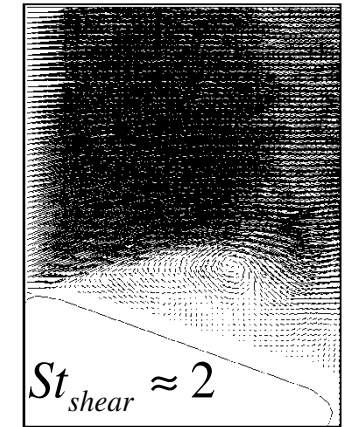
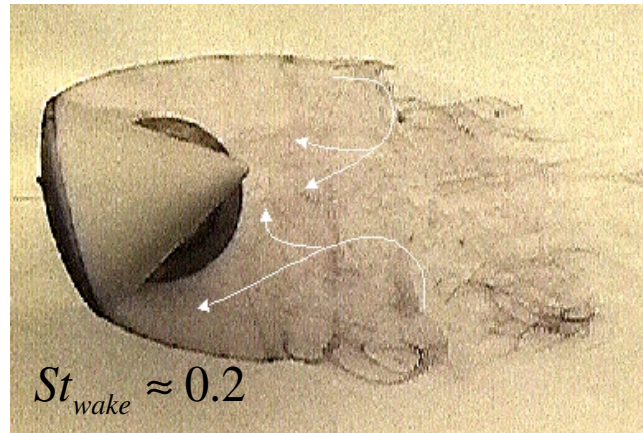
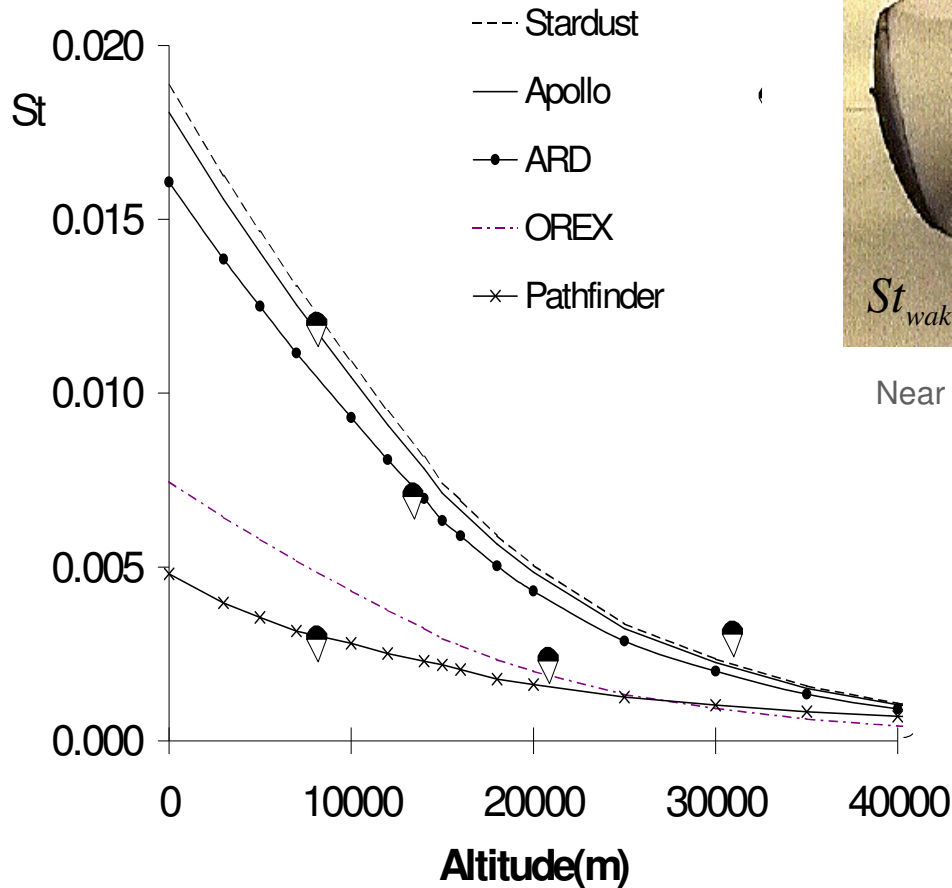
Free oscillation tests: to match the flight Strouhal, wind tunnel usually a light model is required .

$$\left( \frac{I}{\rho_\infty SD^3} \right)_{wt} = \left( \frac{I}{\rho_\infty SD^3} \right)_{ft}$$

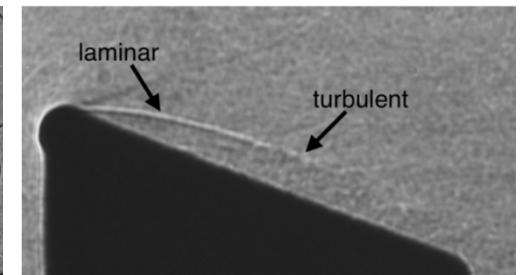
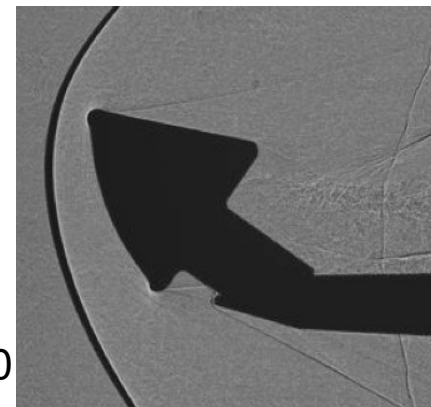
Forced Oscillation tests: Powerful driving mechanism to reach the matching frequency  
Need of light material to avoid large inertial efforts.

$$I_{wt} = I_{flt} \cdot \left( \frac{P_{\infty, wt} T_{\infty, flt} D_{wt}^5}{P_{\infty, flt} T_{\infty, wt} D_{flt}^5} \right)$$

# Non Dimensional Frequencies of Flight and Flow Field



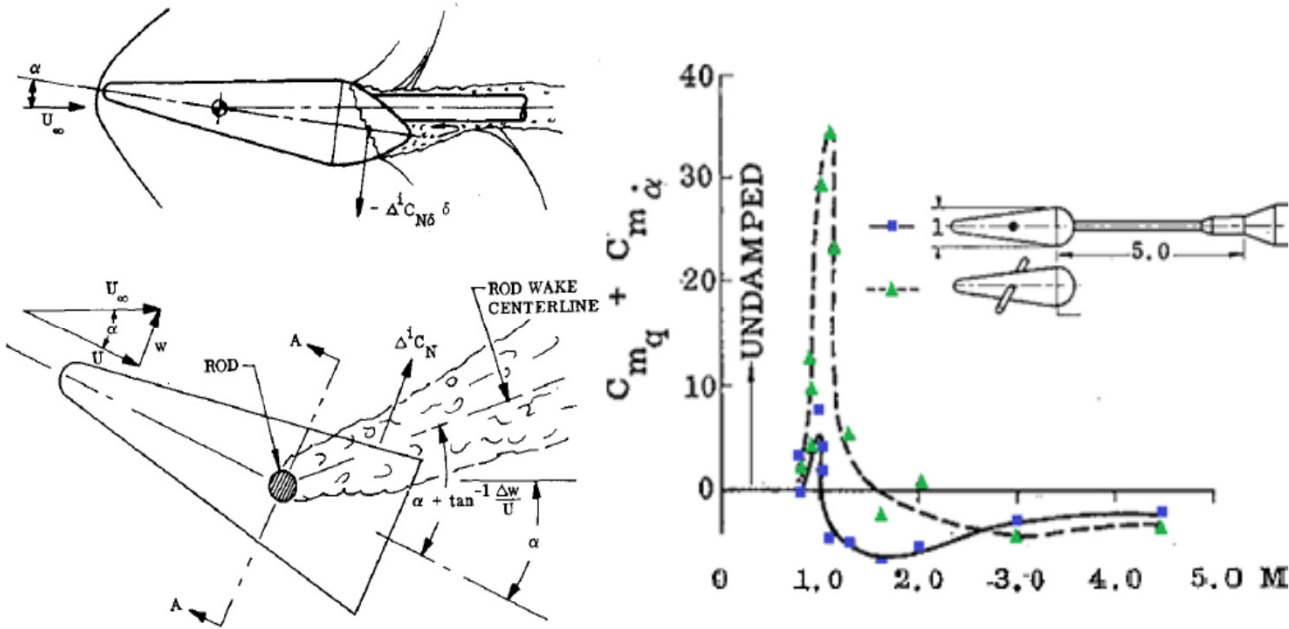
Near wake and shear layer at incompressible flow (Karatekin 2001)



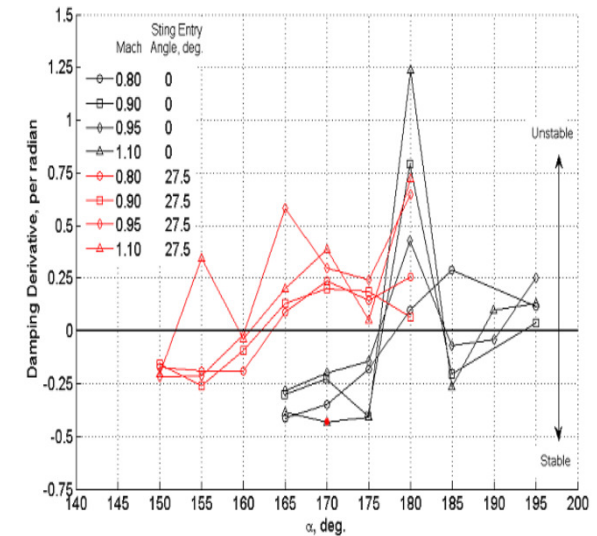
Shadowgraph Indicating wake and Shear Layer Transition at  $M=2$ ,  $Re = 1.75E6$  (Scherijer & Walpot 2011).

There are about one order of magnitude difference between the frequencies associated with flight, wake and shear layer instabilities

# Sting effects



Effect of axial and transverse supports on wake interference (left) and pitch damping (lef) (Reding andEricson 1972)



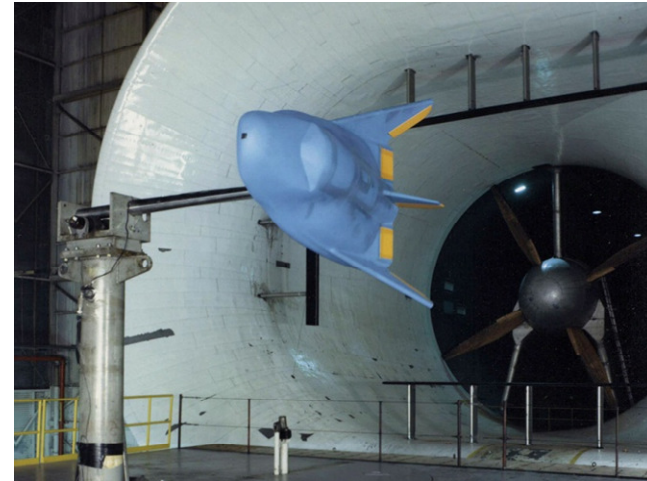
Effect of sting orientation on Orion crew module damping (Owens et al. 2011)

The model support (axial or transverse) perturbs essentially the near wake and affects the model's pressure distribution of the aftbody. Wind tunnel tests show significant influence of support diameter, length, and physical placement on the dynamic stability characteristics.

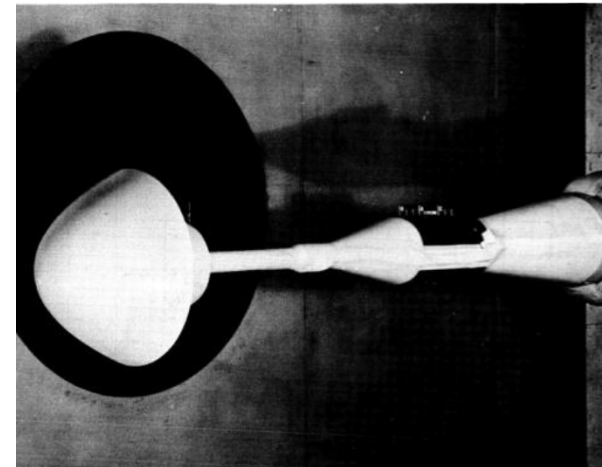
# Forced Oscillation



- Dynamic wind tunnel testing with a forced oscillation setup measures forces, moments as well as the rates of change of these parameters with respect to changing pitch angle or angle of attack.
- In order to capture the dynamic behavior, a motor attached to the sting imparts a one-degree-of-freedom oscillatory motion to the vehicle at a wide range of frequencies and mode shapes.
- The damping response of the vehicle is measured as a function of pitch amplitude, angle of attack, and Mach number.

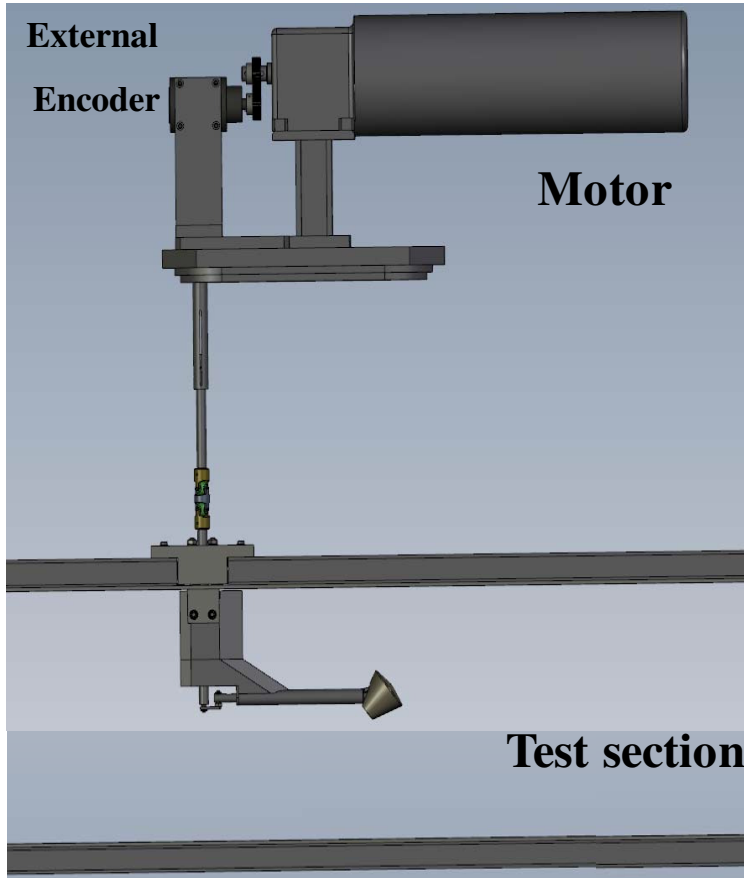


CERV HL-20 Forced Oscillation in Pitch, Credit: NASA Langley



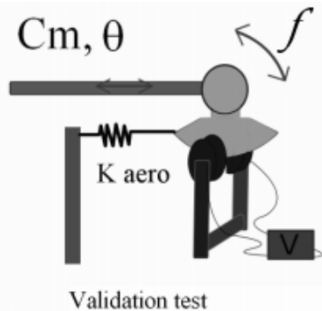
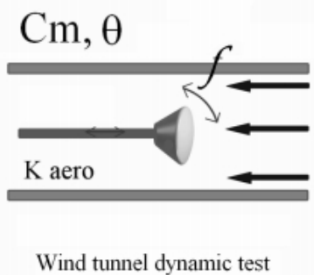
Forced oscillation setup (Moseley et al. 1967).

# Forced Oscillation set-up of VKI



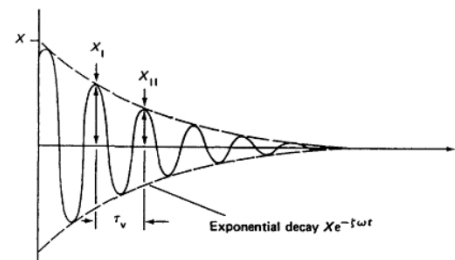
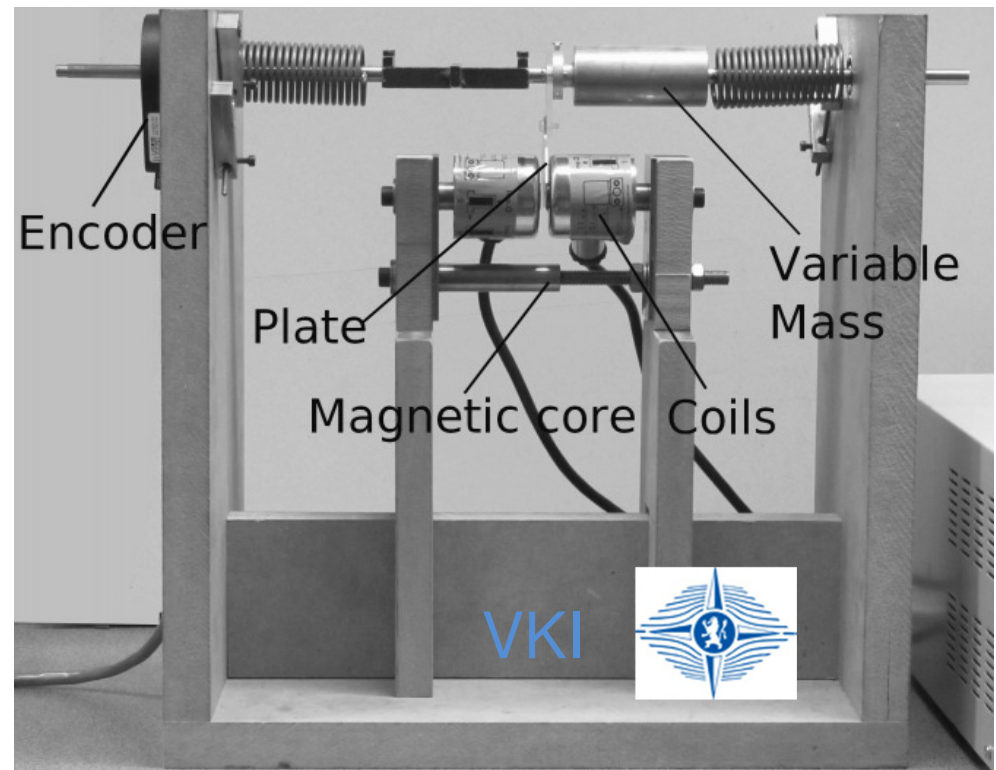
- Forced oscillations set up for Transonic/supersonic tests
- 3-component balance is inserted inside the model. (The CG should be exactly at the center of gravity reduction of the balance and a special interface is required for the calibration and reducing the mechanical damping )

# Forced Oscillation calibration set-up of VKI



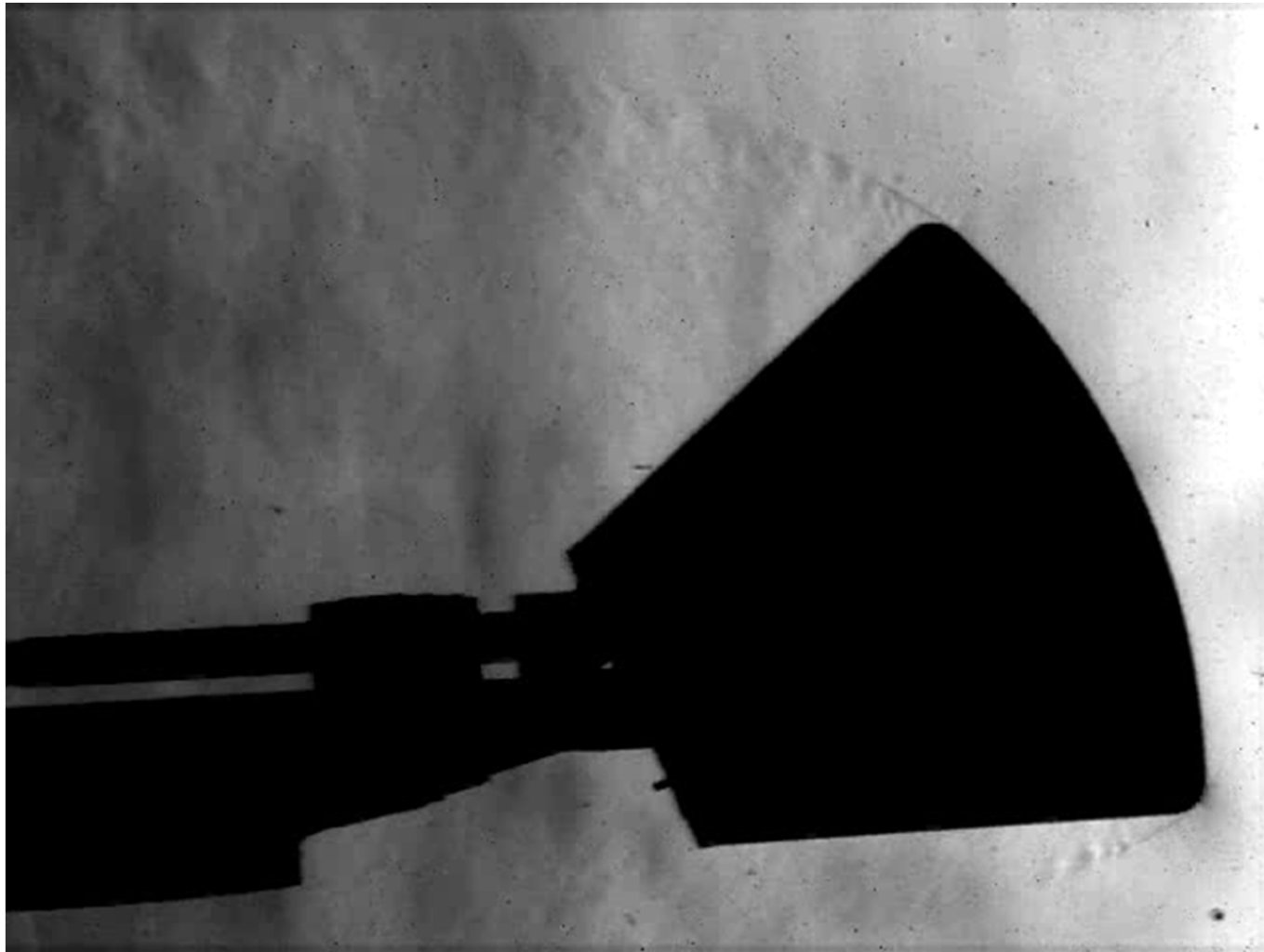
- Definition of the mechanical damping from the ball bearing
- Determination of the magnetic damping (Damping=f (current)) using the logarithmic decrement method and expressed versus amplitude
- Application of the magnetic damping to the existing forced oscillating mechanism
- Data reduction using the energy method

June 15-16, 2013



$$\frac{1}{N} \ln \frac{X_i}{X_{i+N}} = \frac{2\pi\xi}{\sqrt{1-\xi^2}}$$

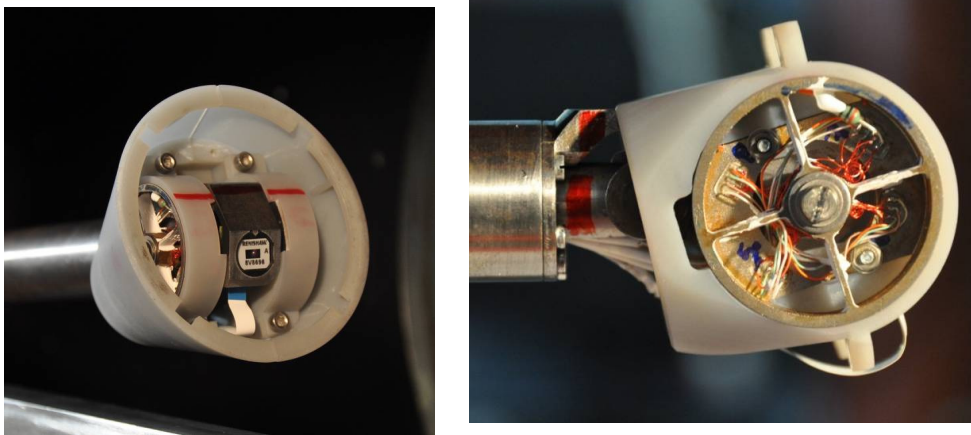
# VKI forced oscillation test



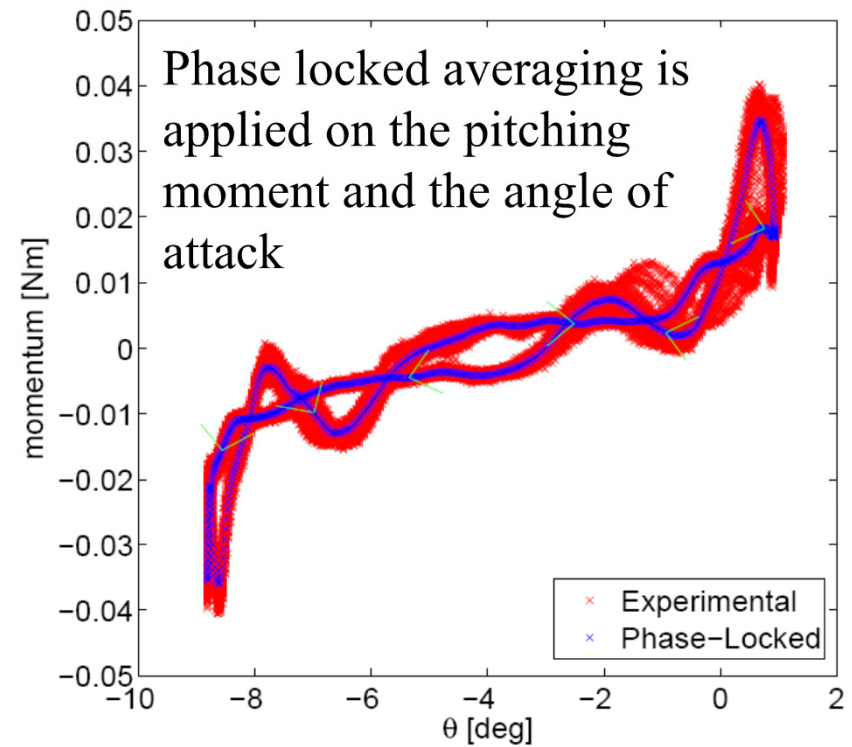
June 15-16, 2013

International Planetary Probe Workshop 10  
Short Course 2013

# Forced Oscillations (VKI)

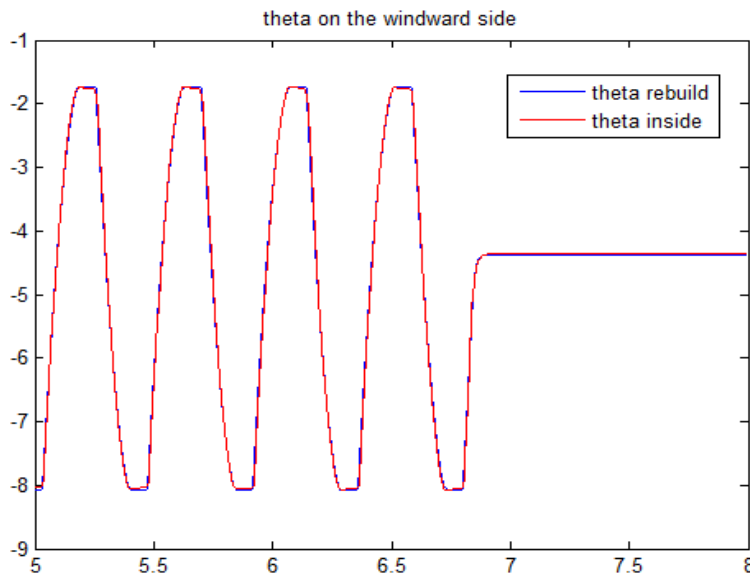


Encoder and the 3 component force and moment balance



Damping is found by the energy method

$$C_{m\dot{\alpha}} + C_{mq} = \frac{\oint C_m d\theta}{\int \dot{\theta}^2 dt} \frac{2U}{D}$$



June 15-16, 2013

International Planetary Probe Workshop 10  
Short Course 2013

VKI



# Free Oscillation



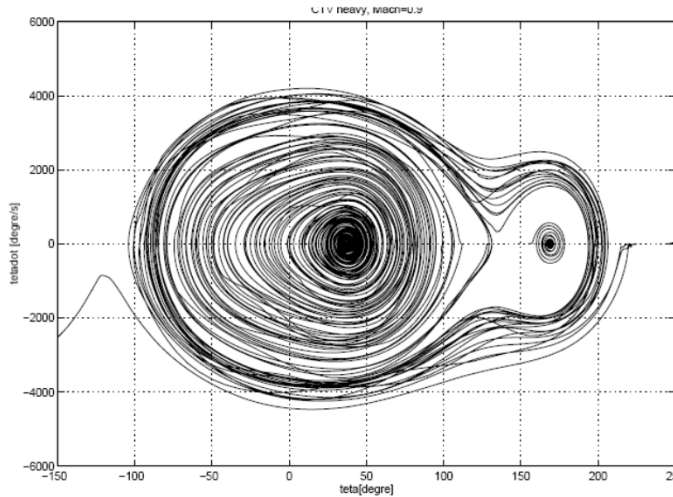
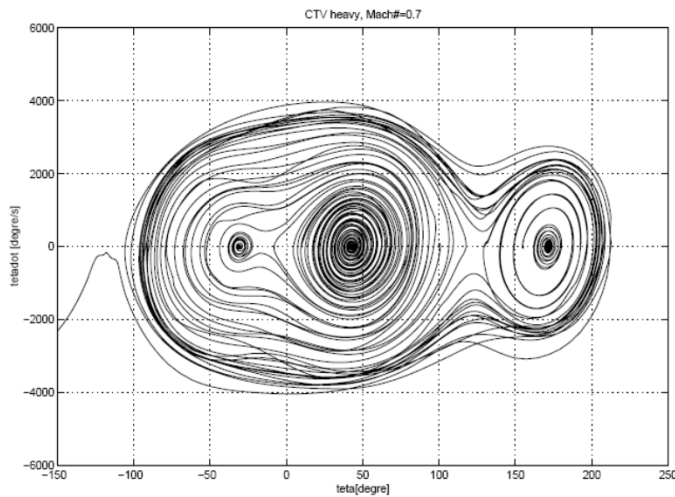
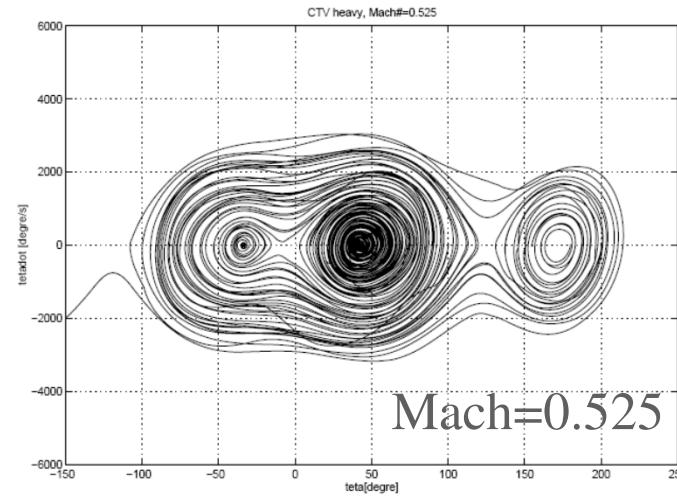
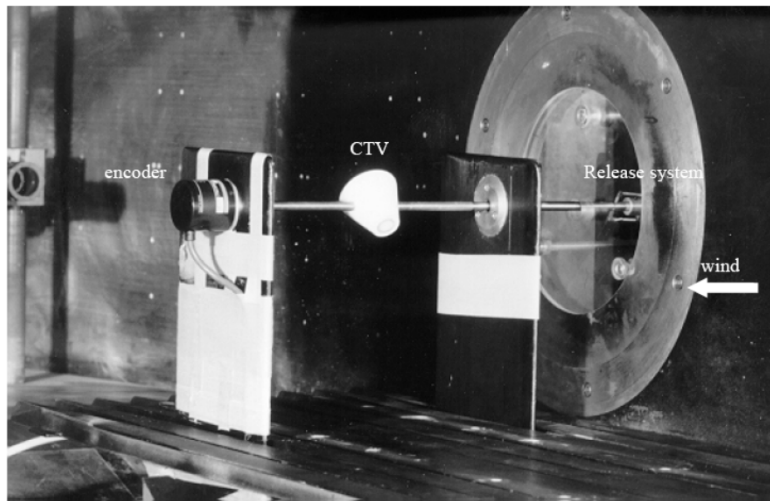
- Free oscillation uses support with low friction bearings that allow the model to pitch freely in response to the aerodynamic forces.
- Following an initial oscillatory perturbation, the vehicle's natural dynamic damping response is monitored.
- By observing the time history of the oscillatory growth or decay, the dynamic aerodynamic coefficients can be determined



June 15-16, 2013

International Planetary Probe Workshop 10  
Short Course 2013

# VKI Free to Tumble Tests



Mach=0.7

Mach=0.9

**Qualitative results:**  
**Mach number effect**

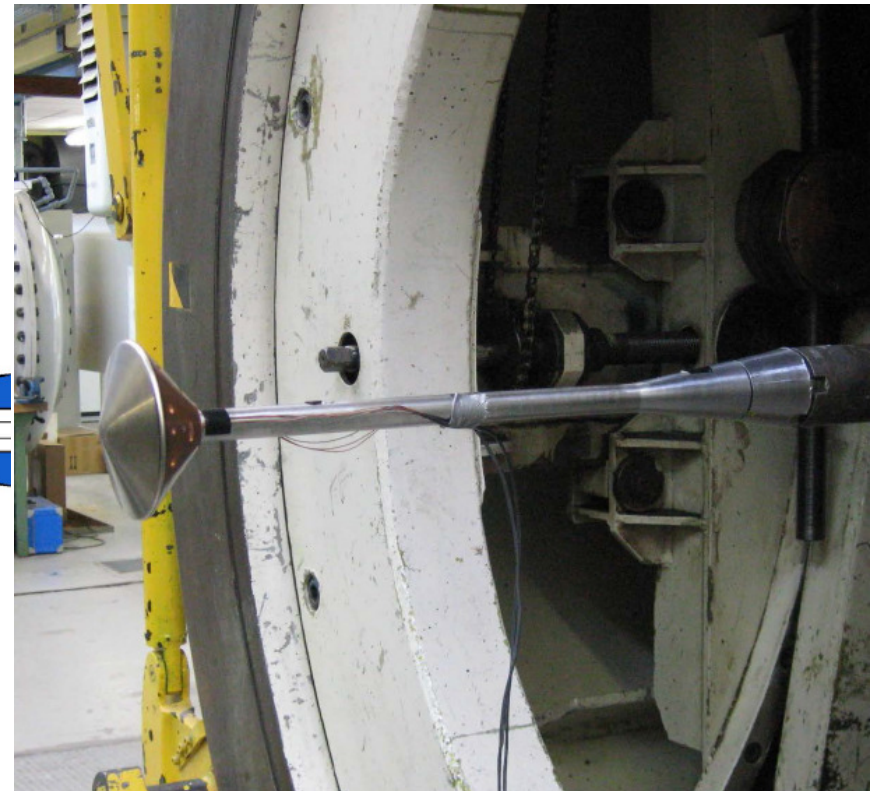
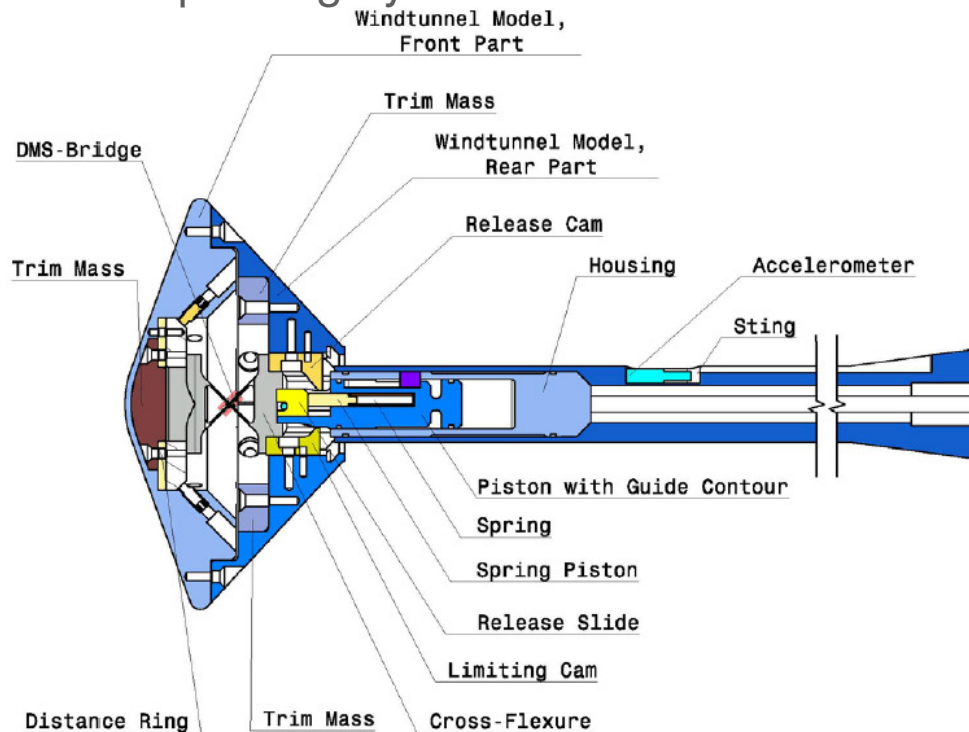
- Stable point around 40° disappears
- Confirmed by static measurement
- Larger stable area with increasing Mach.

# Free Oscillations (DLR)



the model is free to rotate around an axis passing by the CG location

EXPERIMENTAL STUDY OF THE DYNAMIC STABILITY OF THE EXOMARS CAPSULE



Dynamic derivatives of the EXOMARS capsule are estimated via free oscillation method in the Tri-sonic Wind tunnel TMK (DLR) in a Mach number range from 1.8 to 3.5. (Gülhan et al 2011) .

# Free Oscillations (DLR)



$$I_y \ddot{\theta} + (k_y - M_{\dot{\theta}}) \dot{\theta} + (c_y - M_{\theta}) \theta = 0$$

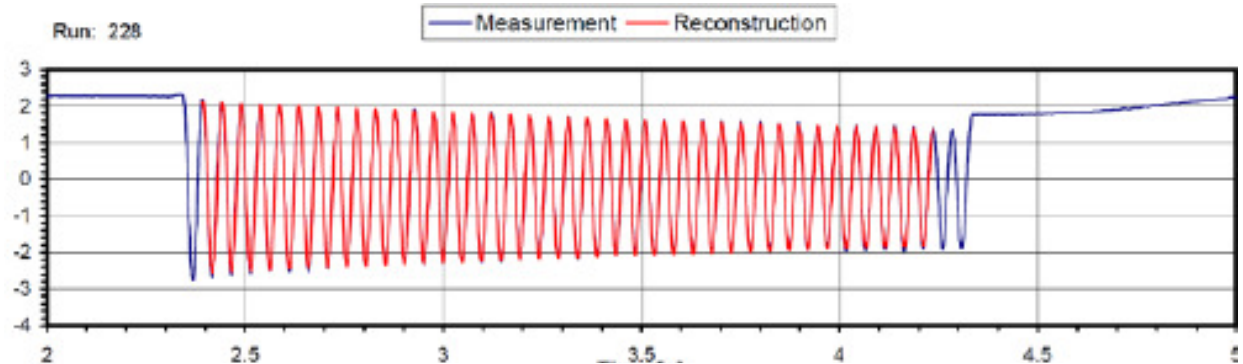
$I_y$ : moment of inertia

$k_y$ : mechanical damping coefficient

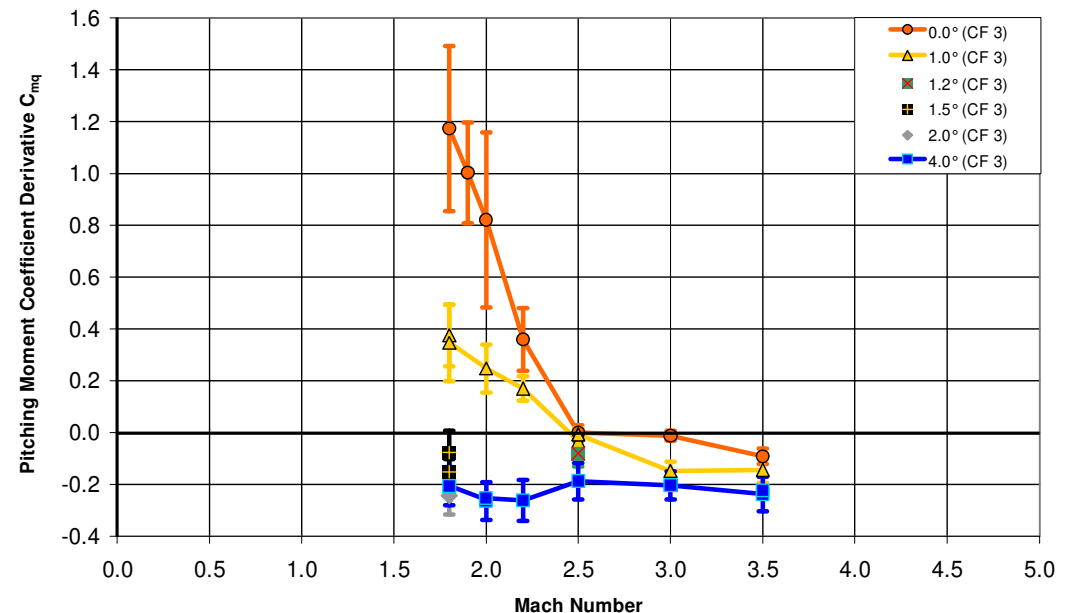
$c_y$ : mechanical stiffness coefficient

$\theta$ : deflection angle

$M$ : aerodynamic moment



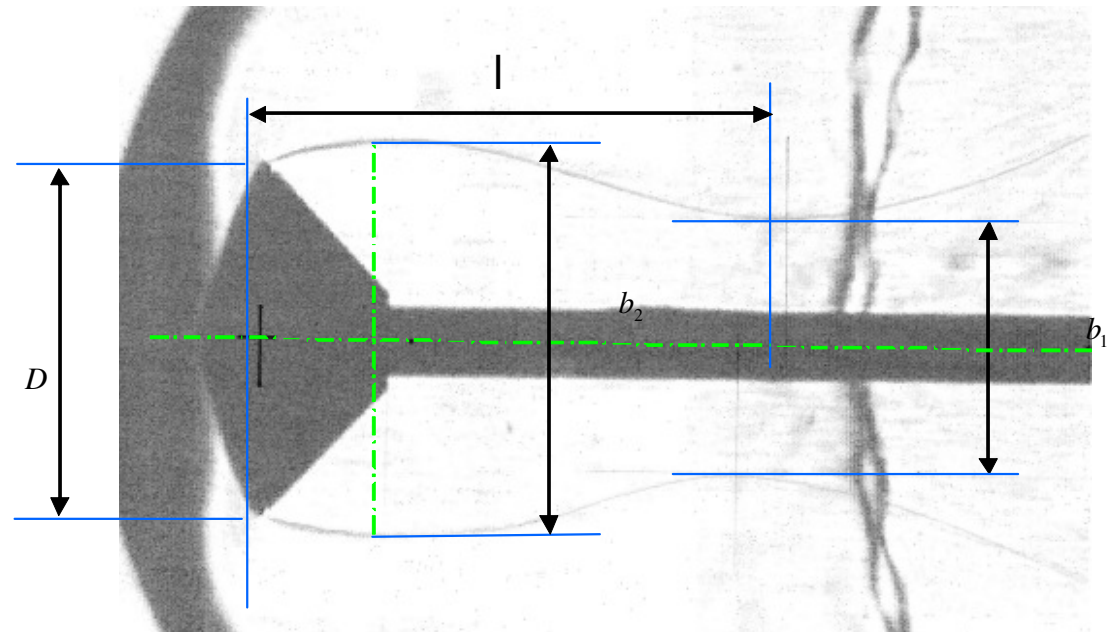
- The method analyses free oscillation of the scaled capsule model fixed on a sting by means of a cross flexure with and without supersonic flow.
- The damping decrement and the free oscillation frequency are calculated on basis of the recorded oscillation data as the nonlinear regression model
- The results show a strong dependency of damping derivatives on the Mach number and angle of attack.



# Effect of the Wake (DLR)



surface	Ma	2.0	3.0	3.5
smooth	$b_2/D$	1.09	0.95	0.93
	$l/D$	n.m.	1.19	1.21
	$c_{mq}$	0.821	-0.012	-0.092
rough	$b_2/D$	1.11	0.98	0.95
	$l/D$	n.m.	1.16	1.18
	$c_{mq}$	0.574	0.236	0.104

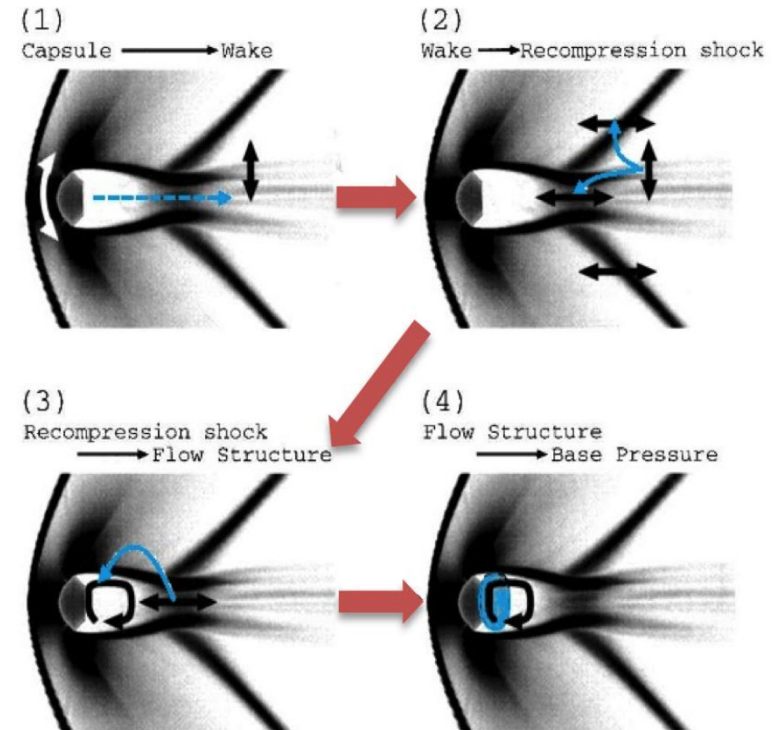


*Characteristics of the wake flow and wake size of EXOMARS depending on the Mach number and surface property (Gülhan et al. 2011)*

# Hysteresis Effects



- Pitching motion causes nonlinearities in the pitching moment slope due to the finite time delay that exists between changes in pitch angle and subsequent changes in the pressure field over the body.
- This hysteresis effect has been cited to describe the mechanism behind dynamic stability.
- It is possible that aftbody pressure field lags the pitching motion and changes in the forebody pressure.

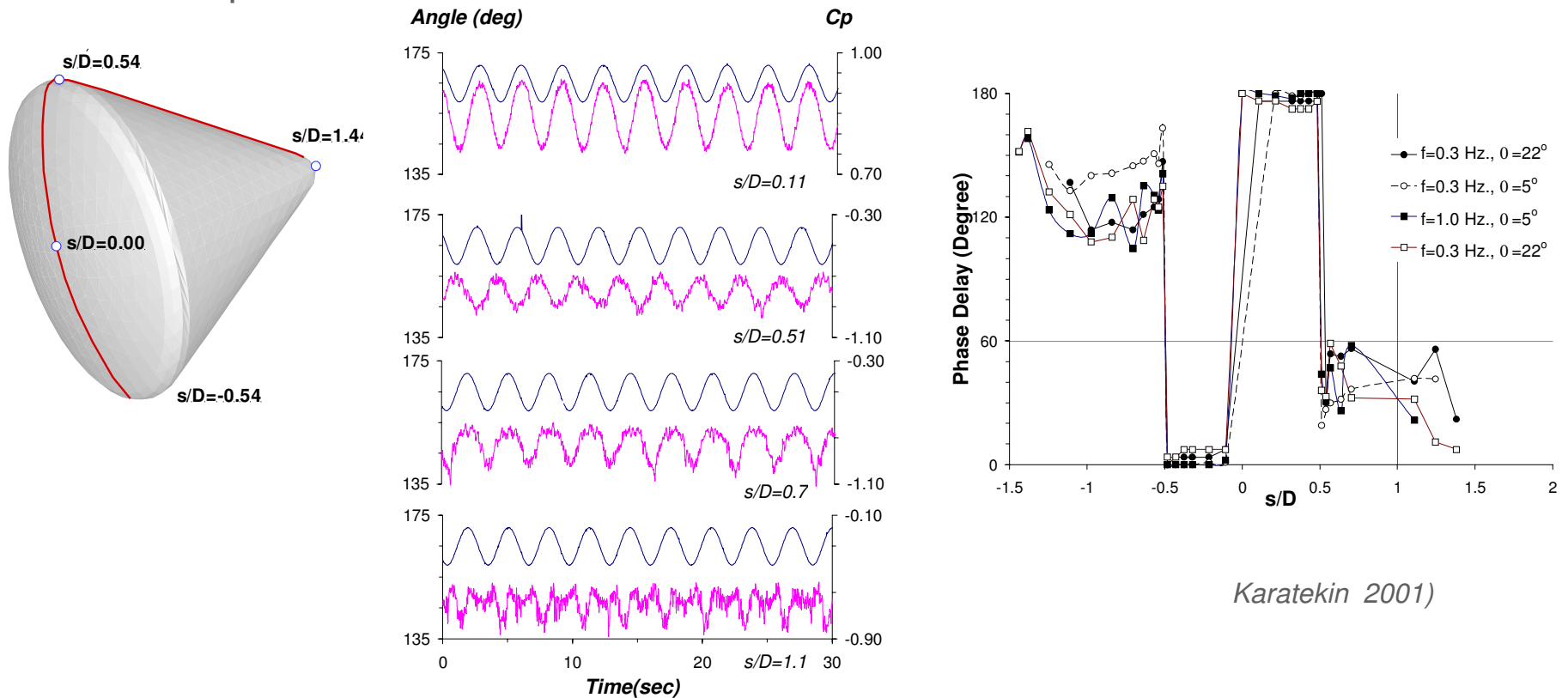


(Teramoto et al. 2001)

# Hysteresis at in Cp



The effect of model's motion on surface pressures is analyzed along the symmetry plane of an Apollo model in forced oscillation (Karatekin 2001). The effect of model's motion on surface pressures is analyzed along the symmetry plane of an Apollo model at incompressible flow.

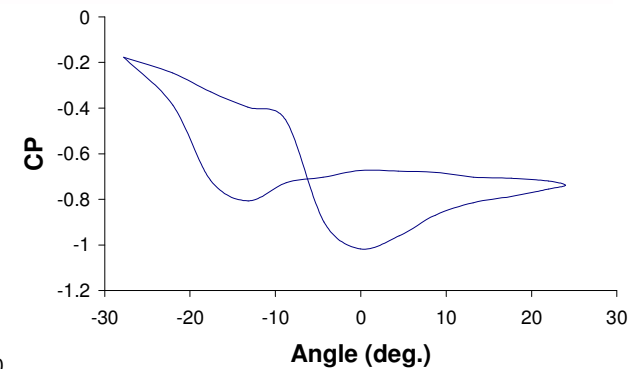
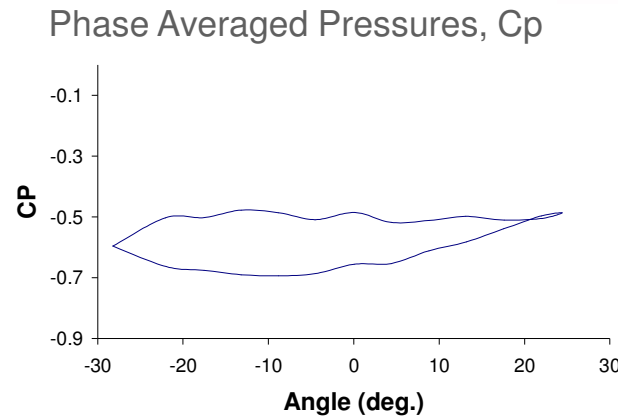
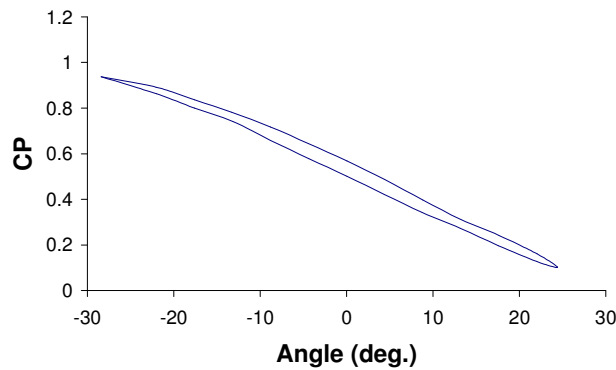
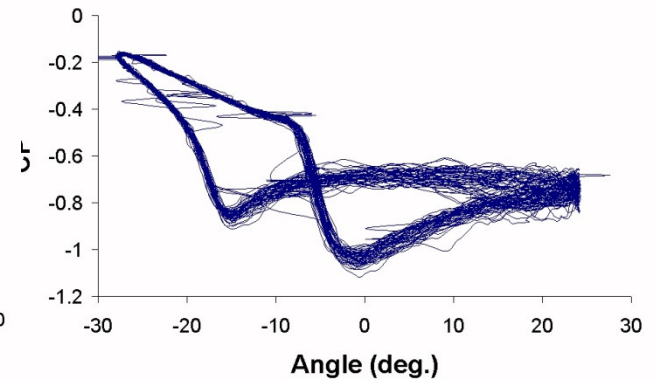
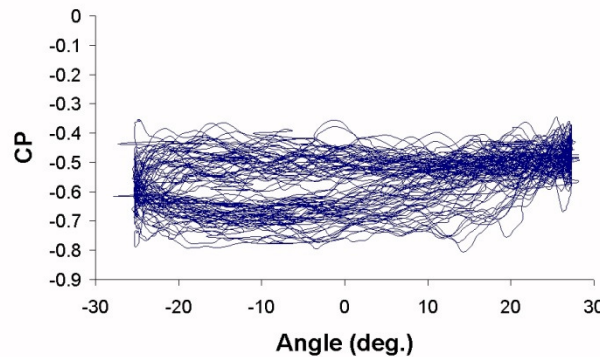
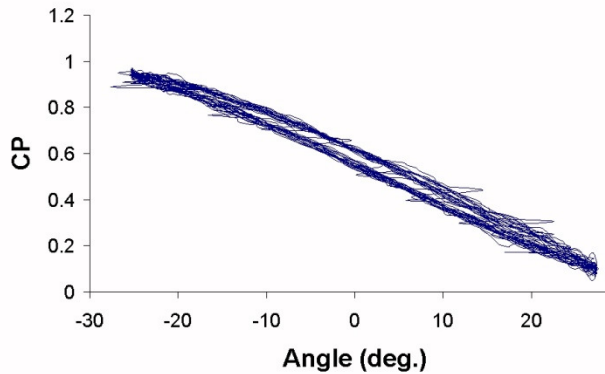


Karatekin 2001)

# Hysteresis at in Cp



Instantaneous pressures, Cp



$\alpha_m=180^\circ$ ,  $f=1$  Hz.,  $\Lambda=22^\circ$   
 $s/D=0.38$

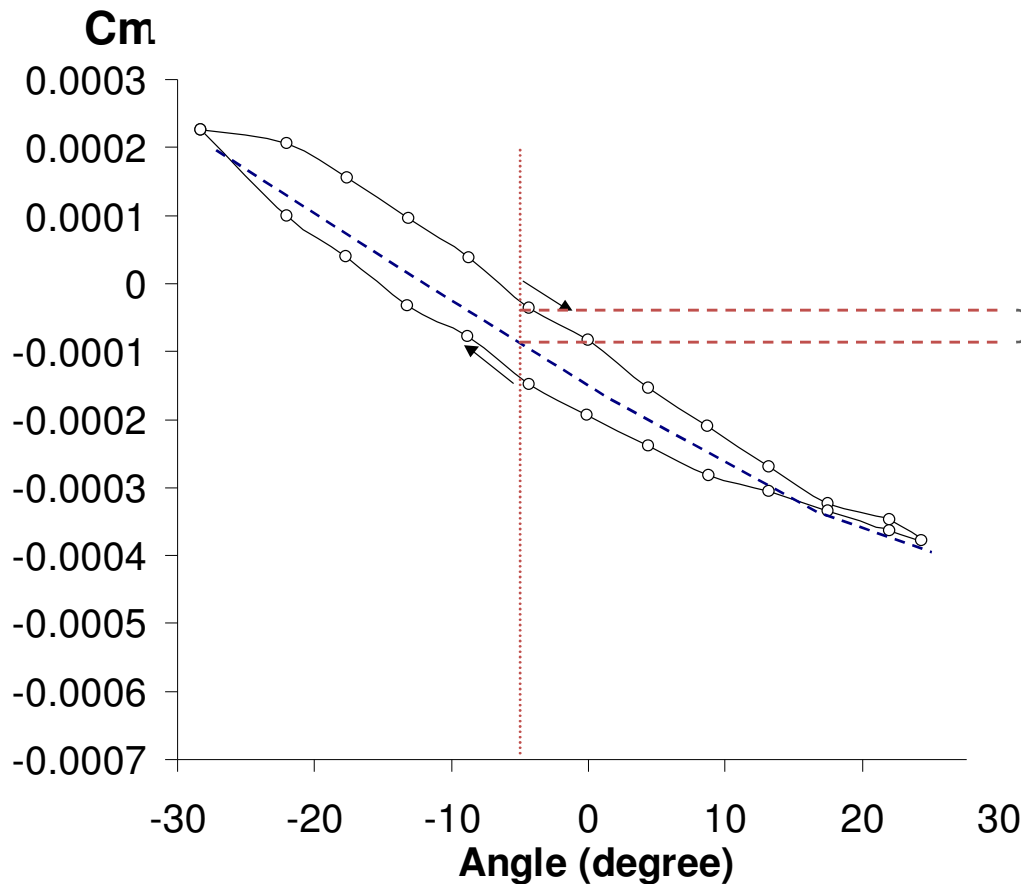
$\alpha_m=180^\circ$ ,  $f=1$  Hz.,  $\Lambda=22^\circ$   
 $s/D=0.70$

$\alpha_m=147^\circ$ ,  $f=1$  Hz.,  $\Lambda=22^\circ$   
 $s/D=0.70$

# Hysterises in Cm



The integration of phase averaged pressures over the body yields hysteresis information



Additional Moment in the direction of the motion !

$$\dot{\theta} > 0$$

$$\Delta C_m > 0$$

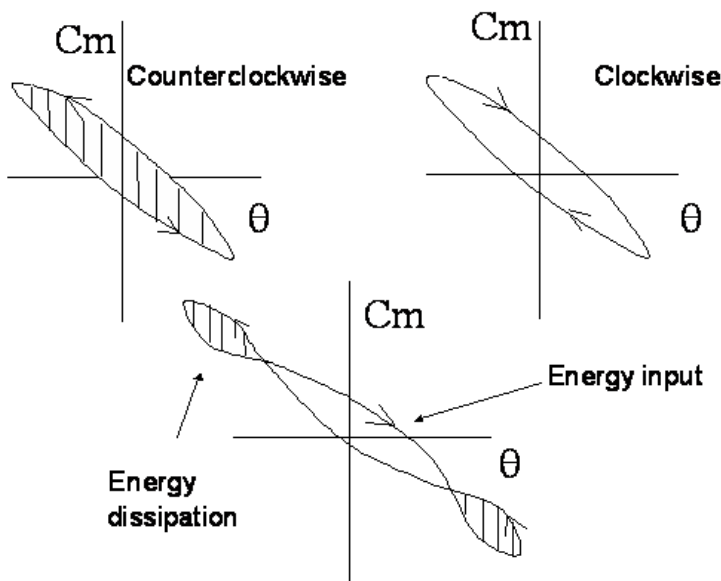
$$\frac{\partial C_m}{\partial \dot{\theta}} > 0 \rightarrow \text{Dynamically unstable}$$

When the hysteresis is such that, the resulting moment during the stroke-up motion is larger than that of the stroke-down motion, the vehicle experiences an additional moment in the direction of its motion. This Time lag effects have the main responsibility for the dynamically unstable motion of entry probes at low speeds.

# Energy Method



The dynamical response of the system can be studied using the energy approach:



The variation of moment curve indicates whether the system has a tendency to amplify (clockwise rotation) or damp-out the angular motion (clockwise rotation).

$$I\ddot{\theta} - (C_{m_q} + C_{m_{\dot{\alpha}}}) \frac{q_{\infty} S D^2}{2U_{\infty}} \dot{\theta} - q_{\infty} S D \frac{\partial C_m}{\partial \theta} \theta = 0$$

$$\oint I \ddot{\theta} \dot{\theta} dt - \oint (C_{m_q} + C_{m_{\dot{\alpha}}}) \frac{q_{\infty} S D^2}{2U_{\infty}} \dot{\theta} \dot{\theta} dt - \oint q_{\infty} S D \frac{\partial C_m}{\partial \theta} \theta \dot{\theta} dt = 0$$

The first term on the left hand side of equation stands for the total energy of the system. The second term is an indication of the work done by the aerodynamic damping. The last term, is associated with the steady state forces. This approach is used to determine the damping coefficients if forced oscillation tests

$$\oint C_m q_{\infty} S D d\theta - \oint (C_{m_q} + C_{m_{\dot{\alpha}}}) \frac{q_{\infty} S D^2}{2U_{\infty}} \dot{\theta} \dot{\theta} dt = 0$$

$$\oint C_m d\theta - \oint (C_{m_q} + C_{m_{\dot{\alpha}}}) \frac{D}{2U_{\infty}} \dot{\theta}^2 dt = 0$$

$$(C_{m_q} + C_{m_{\dot{\alpha}}}) = \frac{\oint C_m d\theta}{\oint \dot{\theta}^2 dt} \frac{2U_{\infty}}{D}$$

This approach has been used to determine the damping coefficients if forced oscillation tests.

# Comparison of Captive Methods



	DOF	Measurements	Model scaling Requirements	Notes
Forced Oscillation	1	aerodynamic coefficients and pitch motion.	<ul style="list-style-type: none"> <li>• CoG shall be coincident with the the center of rotation.</li> <li>• Oscillation frequency shall be representative of flight condition.</li> </ul>	<ul style="list-style-type: none"> <li>• Controllability and repeatability of wide range of reduced frequency parameters</li> <li>• Requires relatively more complex processing and hardware.</li> <li>• Mass scaling is not generally required to obtain representative full scale behavior in the sub scale environment</li> <li>• Average value of the damping over one oscillation cycle.</li> <li>• Noise due to mechanical perturbations</li> <li>• The accuracy depends strain gauge measurements</li> <li>• Presence of sting perturbs the flow.</li> </ul>
Free Oscillation	1	Angular motion as a function of time	<ul style="list-style-type: none"> <li>• cg must be coincident with the center of rotation</li> <li>• the pitch moment of inertia must be scaled properly from the expected full scale vehicle for representative</li> </ul>	<ul style="list-style-type: none"> <li>• Simpler implementation</li> <li>• Direct observation of stability regions.</li> <li>• Sting effects</li> <li>• Average value of the damping over one oscillation cycle.</li> <li>• Damping due to bearing friction must be accurately quantified so that it can be separated from the aerodynamic damping of the vehicle.</li> <li>• Presence of sting perturbs the flow.</li> </ul>

# Comparison of free flight testings



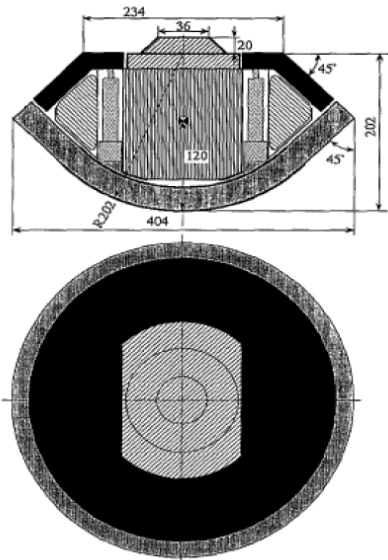
	DOF	Measurements	Model scaling Requirements	Notes
Free Flight	6	Position and oscillation history as a function of time.	Must match $Re$ , $M$ , $I$ , $m$ , $St$ simultaneously	<ul style="list-style-type: none"> <li>• 6 DOF dynamics are obtained by a properly scaled vehicle</li> <li>• Limited observations of the oscillation cycles due to the size of the observable test section within a wind tunnel</li> <li>• Data treatment is cumbersome</li> </ul>
Ballistic	6	Position and oscillation history as a function of time.	Must match $Re$ , $M$ , $I$ , $m$ , $St$ simultaneously	<ul style="list-style-type: none"> <li>• the true, 6 DOF dynamics that are obtained by a properly scaled vehicle</li> <li>• Limited observations of the oscillation cycles due to the size of the observable test section within a wind tunnel</li> <li>• Compared to free flight more pitch cycle observations and thus less uncertainty in data reduction compared to free flight.</li> <li>• Observe the oscillation behavior of a decelerating vehicle..</li> </ul>

# Summary of test methods

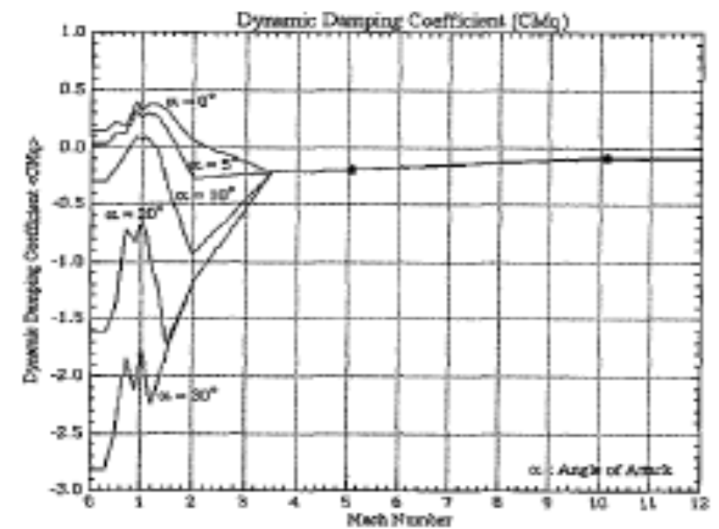
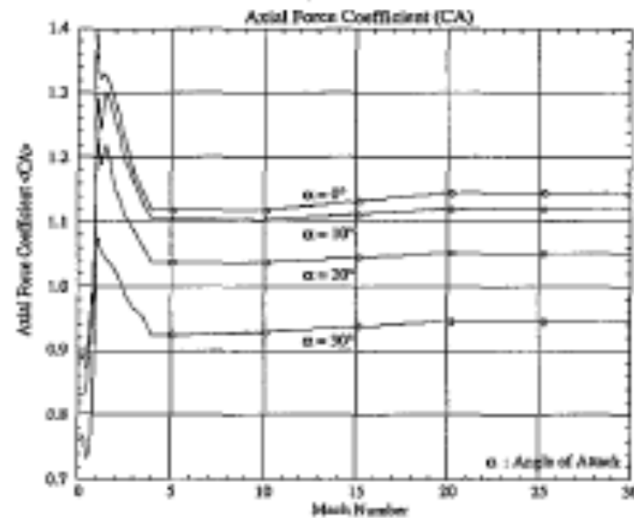
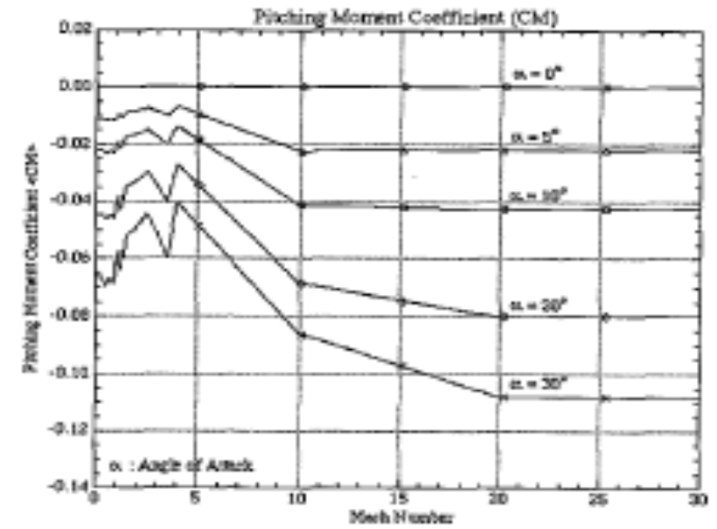
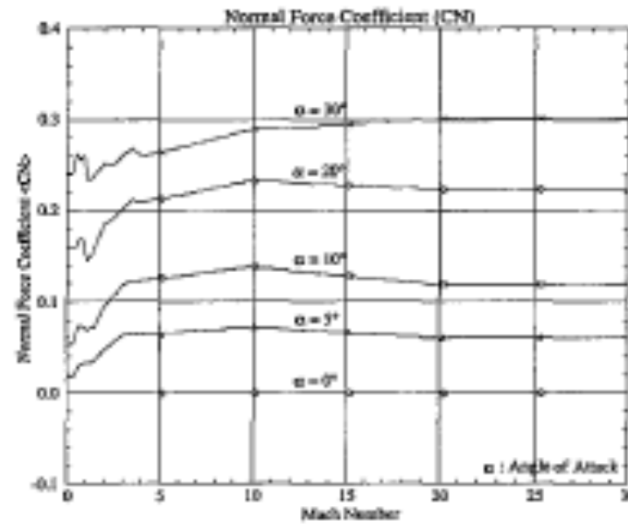


- Captive methods of forced and free oscillation provide single degree of freedom axis behavior and cannot capture real rotational dynamics. Sting effects are the most considerable disadvantage as they are highly dependent on the test conditions, difficult to quantify, and not generally understood.
- Free flight models can recreate the true dynamic performance of the full-scale vehicle to a high degree. However, their greatest shortcomings are in the uncertainty of post processing of the discrete data points to estimate the trajectory and the difficulties in matching scaling parameters and desired initial conditions.

# An aerodynamic database



Attitude Motion and Aerodynamic Characteristics of MUSES-C Reentry Capsule  
*The Institute of Space and Astronautical Science Report SP No. 17 March 3003*

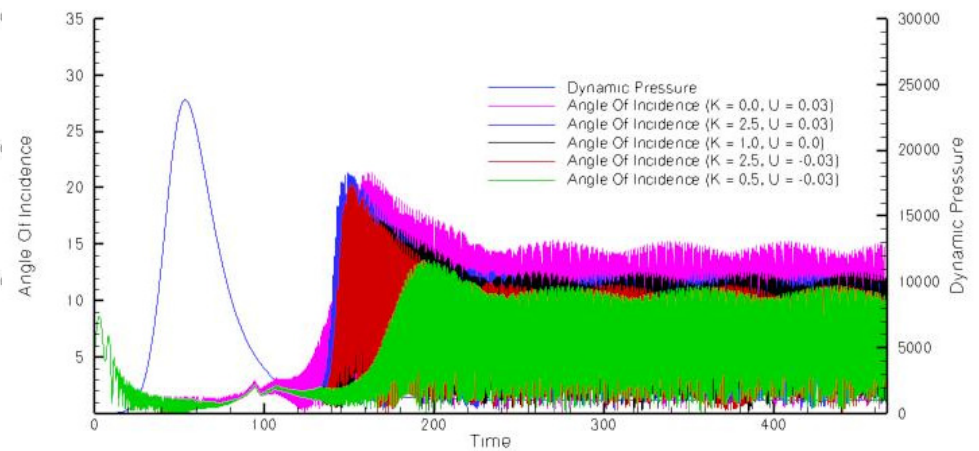
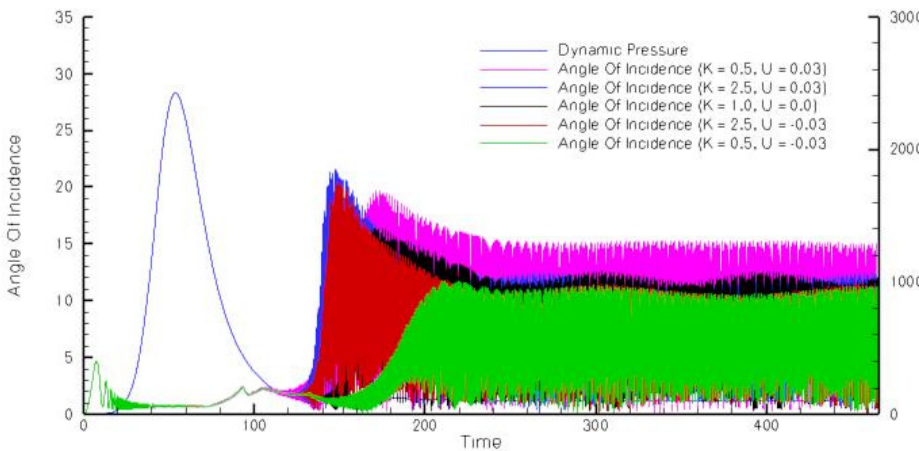
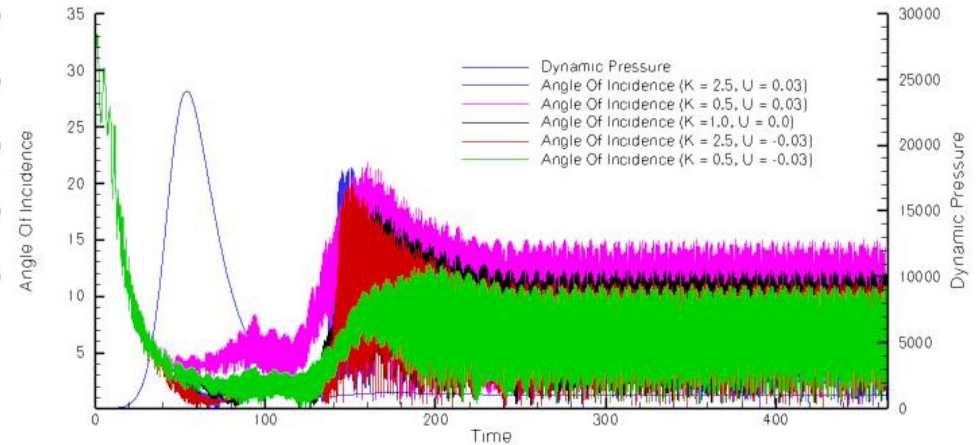
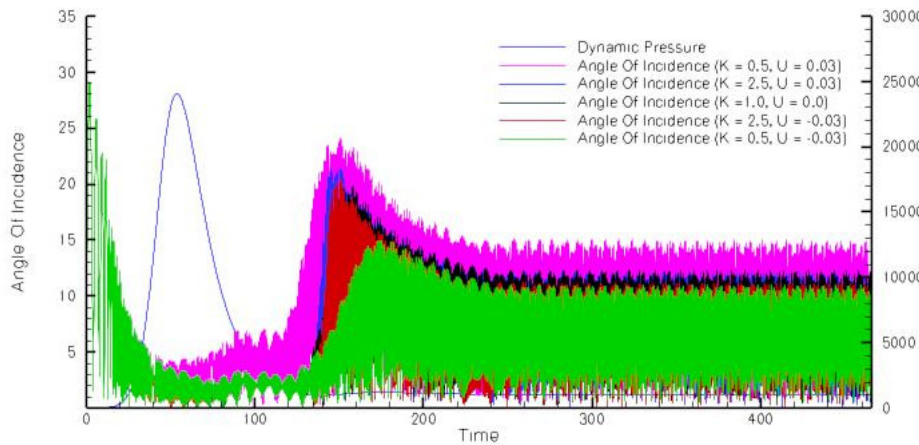


# An aerodynamic database



CA (a / M)	0	0.3	0.5	0.7	0.8	1.0	1.3	2.0	2.5	3.0	3.5	4.0	5.0	10.0	15.0	20.0	25.0	30.0
0	0.891	0.890	0.900	0.923	0.961	1.363	1.326	1.292	1.234	1.179	1.150	1.121	1.119	1.117	1.132	1.146	1.147	1.147
5	0.890	0.888	0.888	0.932	0.985	1.282	1.290	1.277	1.215	1.171	1.141	1.115	1.112	1.110	1.122	1.133	1.134	1.134
10	0.888	0.886	0.876	0.941	1.010	1.200	1.254	1.262	1.196	1.164	1.133	1.109	1.105	1.103	1.112	1.120	1.121	1.121
20	0.831	0.831	0.851	0.930	0.970	1.190	1.194	1.153	1.114	1.088	1.062	1.037	1.037	1.037	1.046	1.052	1.052	1.052
30	0.768	0.767	0.735	0.755	0.826	1.071	1.054	1.027	0.995	0.968	0.956	0.925	0.924	0.927	0.937	0.945	0.945	0.946
CN (a / M)	0	0.3	0.5	0.7	0.8	1.0	1.3	2.0	2.5	3.0	3.5	4.0	5.0	10.0	15.0	20.0	25.0	30.0
0	0.000	0.000	0.000	0.000	0.000	0.000	0.000	0.000	0.000	0.000	0.000	0.000	0.000	0.000	0.000	0.000	0.000	0.000
5	0.018	0.018	0.024	0.029	0.032	0.033	0.034	0.046	0.055	0.062	0.063	0.064	0.065	0.072	0.066	0.060	0.061	0.060
10	0.053	0.057	0.067	0.072	0.071	0.069	0.071	0.097	0.109	0.119	0.121	0.122	0.126	0.138	0.129	0.120	0.119	0.120
20	0.161	0.161	0.162	0.168	0.162	0.149	0.155	0.185	0.192	0.201	0.211	0.211	0.215	0.232	0.229	0.224	0.224	0.223
30	0.241	0.242	0.260	0.256	0.258	0.247	0.238	0.251	0.252	0.261	0.268	0.260	0.264	0.289	0.296	0.301	0.301	0.301
Cm (a / M)	0	0.3	0.5	0.7	0.8	1.0	1.3	2.0	2.5	3.0	3.5	4.0	5.0	10.0	15.0	20.0	25.0	30.0
0	0.000	0.000	0.000	0.000	0.000	0.000	0.000	0.000	0.000	0.000	0.000	0.000	0.000	0.000	0.000	0.000	0.000	0.000
5	-0.011	-0.011	-0.011	-0.012	-0.012	-0.010	-0.010	-0.008	-0.007	-0.008	-0.009	-0.006	-0.009	-0.022	-0.022	-0.021	-0.022	-0.022
10	-0.021	-0.022	-0.023	-0.022	-0.023	-0.020	-0.019	-0.016	-0.014	-0.017	-0.019	-0.014	-0.017	-0.040	-0.042	-0.042	-0.042	-0.043
20	-0.044	-0.044	-0.045	-0.045	-0.045	-0.041	-0.039	-0.032	-0.030	-0.035	-0.039	-0.028	-0.034	-0.067	-0.074	-0.079	-0.080	-0.080
30	-0.066	-0.066	-0.069	-0.067	-0.068	-0.059	-0.059	-0.049	-0.045	-0.052	-0.059	-0.044	-0.048	-0.084	-0.097	-0.107	-0.108	-0.108
Cmq (a / M)	0	0.3	0.5	0.7	0.8	1.0	1.3	2.0	2.5	3.0	3.5	4.0	5.0	10.0	15.0	20.0	25.0	30.0
0	0.148	0.136	0.218	0.206	0.303	0.335	0.366	0.075	-0.038	-0.129	-0.225	-0.214	-0.192	-0.103	-0.098	-0.098	-0.098	-0.098
5	0.028	0.031	0.089	0.120	0.220	0.262	0.251	-0.259	-0.260	-0.242	-0.225	-0.216	-0.198	-0.097	-0.098	-0.098	-0.098	-0.098
10	-0.300	-0.277	-0.151	-0.022	0.043	0.089	-0.005	-0.909	-0.701	-0.470	-0.224	-0.212	-0.186	-0.091	-0.098	-0.098	-0.098	-0.098
20	-1.606	-1.573	-1.282	-0.744	-0.788	-0.666	-1.206	-1.160	-0.846	-0.532	-0.225	-0.214	-0.193	-0.091	-0.104	-0.104	-0.104	-0.104
30	-2.817	-2.764	-2.391	-1.876	-2.010	-1.813	-2.067	-1.199	-0.867	-0.538	-0.236	-0.222	-0.194	-0.097	-0.098	-0.098	-0.098	-0.098

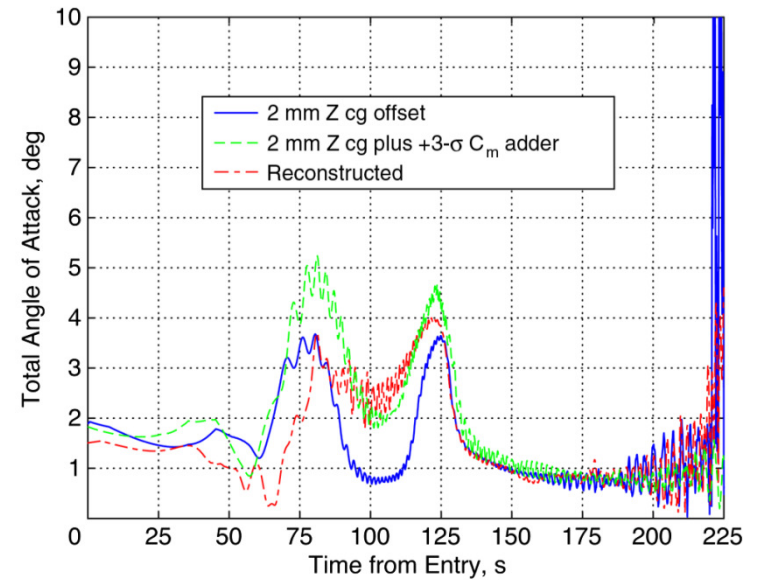
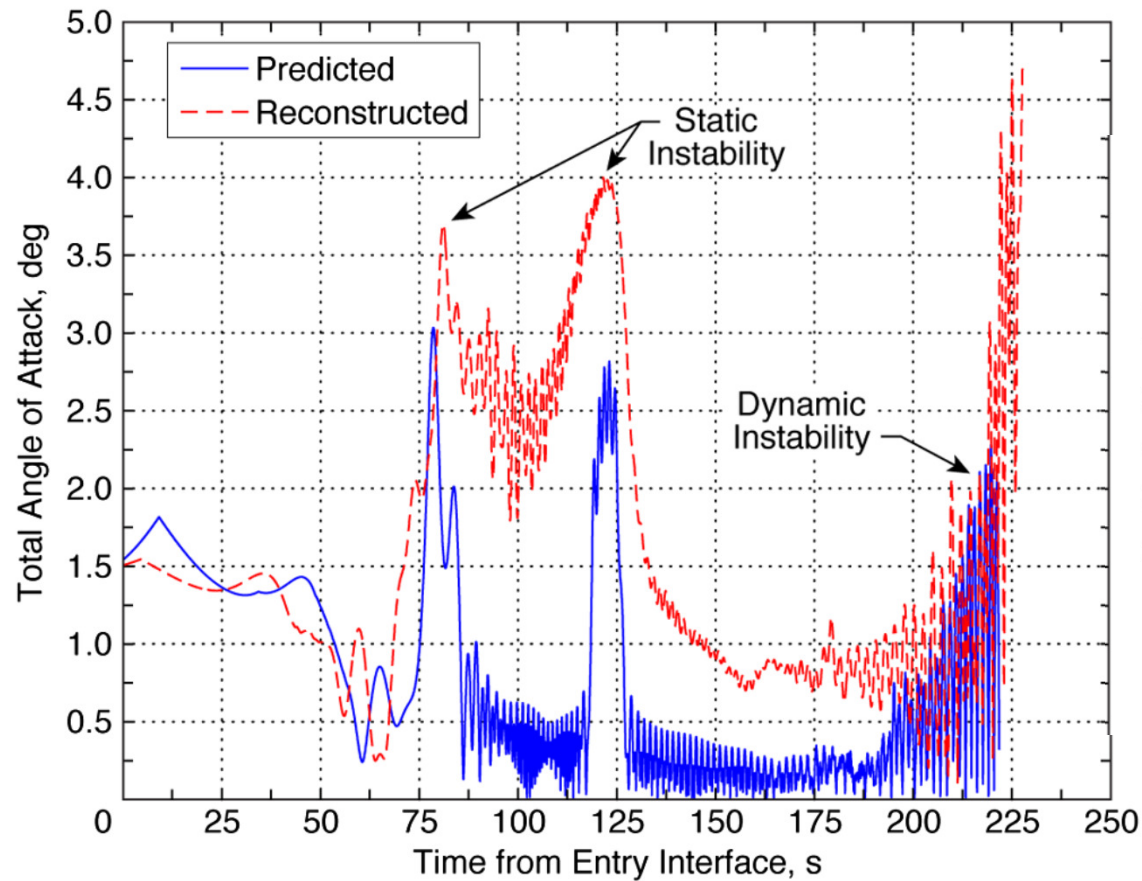
# 6 DoF Trajectory simulations



June 15-16, 2013

International Planetary Probe Workshop 10  
Short Course 2013

# Phoenix EDL Performances



Desai et al. 2011

# Reading Material



- M. Baillion, “Blunt Bodies Dynamic Derivatives,” AGARD-R-808 – Capsule Aerothermodynamics, 1995.
- D. Bird, “Stability of Ballistic Reentry Bodies,” NACA RM L-58, 1958.
- Karatekin O. “Aerodynamics of a Planetary entry capsule at low speeds) Ph.D Thesis, VKI/ULB, Belgium 2001.
- L. E. Ericsson and J. P. Reding, “Re-Entry Capsule Dynamics,” Journal of Spacecraft and Rockets, vol. 8, no. 6, 1971.
- G. T. Chapman and L. A. Yates, “Dynamics of Planetary Probes : Design and Testing Issues,” AIAA 1998-0797, 1998.
- S. Teramoto, K. Fujii, and K. Hiraki, “Numerical Analysis of Dynamic Stability of a Reentry Capsule at Transonic Speeds,” AIAA 98-4451, AIAA Journal 39-4, vol. 39, no. 4, pp. 646-653, Apr. 2001.
- Kazemba et al. “Survey of Blunt Body Dynamic Stability in Supersonic Flow” AIAA-2012-4509, 2012.